

THE UNIVERSITY OF MICHIGAN

7140-1-T

STUDY AND INVESTIGATION OF A UHF-VHF ANTENNA

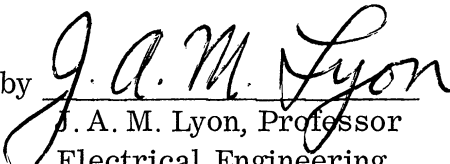
Interim Engineering Report
February through 30 June 1965

July 1965

Prepared by

J. A. M. Lyon, N. G. Alexopoulos, C-C Chen, A. M. Kazi
and G. G. Rassweiler

Approved by


J. A. M. Lyon, Professor
Electrical Engineering

Contract No. AF 33(615)-2102
Project 6278, Task 627801
O. E. Horton, Project Monitor

Air Force Avionics Laboratory AVWE
Research and Technology Division, AFSC
Wright-Patterson Air Force Base, Ohio 45433

FOREWORD

This report was prepared by The University of Michigan under USAF Contract No. AF 33(615)-2102. The contract was initiated under Project 6278, "VHF-UHF Antenna Study," Task 627801. This was administered under the direction of the Electronic Warfare Division, Air Force Avionics Laboratory, Research and Technology Division, Air Force Systems Command at Wright-Patterson Air Force Base, Mr. Olin E. Horton, Project Engineer (AVWE).

TABLE OF CONTENTS

| | Page |
|--|------|
| LIST OF FIGURES | vi |
| ABSTRACT | viii |
| I INTRODUCTION | 1 |
| II TRAVELING WAVE ANTENNAS WITH FERRITE LOADING | 2 |
| 2.1 Conical Log Spiral | 2 |
| 2.2 Ferrite-Loaded Helical Antennas | 3 |
| 2.2.1 Bifilar Helical Antennas | 7 |
| 2.2.2 Monofilar Helices | 16 |
| III FERRITE SLOT ARRAYS | 21 |
| 3.1 Ferrite Waveguide Preliminary Tests | 21 |
| 3.2 Preliminary Non-resonant Array Tests | 21 |
| 3.3 Magnetic Bias Control of Ferrite Array | 25 |
| IV ENERGY TRANSFER TO FERRITE SLAB | 26 |
| 4.1 Analysis | 26 |
| 4.2 Experiments on Energy Transfer and Radiation | 35 |
| V SLOT ANTENNAS WITH RIDGES OR IRISES | 37 |
| 5.1 Assumptions of the Study | 37 |
| 5.2 Solid Ferrite Loaded Antenna | 37 |
| 5.3 Loaded Slot Antenna with Irises | 41 |
| 5.4 Ridged Loaded Slot Antennas | 46 |
| 5.5 Conclusions and Summary | 49 |
| VI FERRITE MATERIALS | 56 |
| VII FUTURE EFFORT | 60 |
| ACKNOWLEDGEMENTS | 61 |
| REFERENCES | 62 |

LIST OF FIGURES

| | | <u>Page</u> |
|-----|--|-------------|
| 1 | Conical Spiral (No. 200) Loaded with Solid Ferrite Bars | 4 |
| 2 | Impedance Diagram of Solid-Ferrite Loaded Conical Helix Antenna. Bottom Half of Cone Shell Loaded. | 5 |
| 3 | Impedance Diagram of Solid-Ferrite Loaded Conical Helix Antenna. Entire Conical Shell Loading. | 6 |
| 4 | Bifilar 4" Helix with Balsa Wood Core and Cap. | 8 |
| 5 | Fiberglass-Epoxy Tube Form for Helices | 9 |
| 6 | Loading Diagram: Bifilar Helix (No. 213) Full Core Loading. | 11 |
| 7 | Loading Diagram: Bifilar Helix (No. 213) Layer Loading. | 12 |
| 8 | Loading Diagram: Bifilar Helix (No. 213) Layer Loading Plus End Cap. | 13 |
| 9 | Bifilar Helix (No. 213) Antenna Patterns. Loaded vs Unloaded. | 14 |
| 10 | Bifilar Helix (No. 213) Antenna Patterns. Unloaded vs Loaded. | 15 |
| 11 | Monofilar 4" Helix with Small Tube for Center Conductor. | 17 |
| 12 | 4" Monofilar Helix (No. 215) $ E_{\theta} ^2$ Linear Power. Unloaded vs Loaded. | 18 |
| 13 | 4" Monofilar Helix (No. 215) $ E_{\phi} ^2$ Linear Power. Unloaded vs Loaded. | 19 |
| 14 | Proposed Mechanical Configuration for Waveguide Test. | 22 |
| 15 | Experimental Details to Determine Insertion Loss of Waveguide. | 23 |
| 16 | Simplified Diagram of 9-slot Ferrite Loaded Waveguide Array. | 24 |
| 17 | Coupled Ferrite Slab Antenna | 27 |
| 18 | Energy Transfer Between Two Coupled Lines. | 33 |
| 19a | Impedance Diagram of Slot Antenna Loaded Entirely with Solid Ferrite. | 38 |
| 19b | Impedance Diagram of Slot Antenna Loaded Entirely with Solid Ferrite. Double Stub Tuner Used. | 40 |
| 20a | Impedance Diagram of Solid Ferrite Loaded Slot Antenna with Iris. | 42 |
| 20b | Impedance Diagram of Solid Ferrite Loaded Slot Antenna with Iris. Double Stub Tuner Used. | 43 |

LIST OF FIGURES
(continued)

| | | <u>Page</u> |
|-----|---|-------------|
| 20c | Impedance Diagram of Solid Ferrite Loaded Slot Antenna with Iris. | 44 |
| 20d | Impedance Diagram of Solid Ferrite Loaded Slot Antenna with Iris. | 45 |
| 21a | Impedance Diagram of Solid Ferrite Loaded Slot Antenna with Ridges. | 47 |
| 21b | Impedance Diagram of Solid Ferrite Loaded Slot Antenna with Ridges. | 48 |
| 21c | Impedance Diagram of Solid Ferrite Loaded Slot Antenna with Ridges. | 50 |
| 21d | Impedance Diagram of Solid Ferrite Loaded Slot Antenna with Ridges. | 51 |
| 21e | Impedance Diagram of Solid Ferrite Loaded Slot Antenna with Ridges. | 52 |
| 21f | Impedance Diagram of Solid Ferrite Loaded Slot Antenna with Ridges. | 53 |
| 21g | Impedance Diagram of Solid Ferrite Loaded Slot Antenna with Ridges. | 54 |
| 22 | Q and μ' For Various Ferrites. | 57 |

ABSTRACT

This report covers the preliminary efforts on the experimental and analytical studies involving the loading of various types of antennas with ferrite material. Major emphasis has been placed upon improvements of conical log spiral antennas through the use of ferrite loading techniques. With this in mind, a series of basic studies on the ferrite loading of helices has been made. These studies indicate the effect of thickness and placement of ferrite material. Data are given showing the shifting of the operating frequency due to the introduction of ferrite material. Also some information is given on the bandwidth for these study type antennas.

A preliminary effort has been devoted to the design of simple slot arrays using ferrite material with provision for magnetic control of these arrays.

This technical report has been reviewed and is approved.

I
INTRODUCTION

The contract effort described here is a continuation of a previous effort⁺ showing the possibility of improved performance for UHF-VHF antennas with ferrite loading. The early effort in this contract period has been to clearly show the importance of the amount of ferrite loading as well as the placement of ferrite loading with respect to traveling wave antennas such as the conical log spiral antenna. The preliminary experiments described are on helices since the study of the helix antenna is often considered to be a good analytical starting point for the study of the spiral log conical antenna. Anticipated effort on this project will include the analytical study of the loaded conical log spiral antenna.

Work has been initiated on the log zig-zag antenna with ferrite loading. Also, effort has been expended which resulted in a preliminary design of a ferrite-loaded waveguide test, and a preliminary design on ferrite slot arrays using this waveguide one of which is capable of magnetic control. Early work on previous contracts has shown that magnetic bias can shift the center of frequency of the operating band of an antenna. The magnetic control of the slot arrays will make use of the change of the incremental permeability of the ferrite material, thus providing shifts in the phasing of the various elements.

⁺ AF 33(657)-10607, Air Force Avionics Laboratory.

II

TRAVELING WAVE ANTENNAS WITH FERRITE LOADING

The analytical work so far has been to review available analysis of helices and conical log spiral antennas. Such analysis has for the most part, been on unloaded types of antennas. Extensions of this analysis to ferrite loaded conical log spiral antennas have not progressed to a form suitable for inclusion in this report. Pertinent references useful for this type of analysis are listed at the end of this report. Additions to the analysis may be based on a mathematical model selected after detailed information upon the ferrite loading of helices is available. The conical log spiral antenna could also properly be called the conical log helix antenna throughout this report; both terminologies are used.

Specific types chosen for ferrite loading of traveling wave antennas include the conical log spiral antenna and the log zig-zag antenna. These choices were made because one of them represents an often used circularly polarized antenna, whereas the other is a linear polarized antenna.

2.1 Conical Log Spiral

The conical log spiral antenna with ferrite loading is being considered both from the experimental and analytical viewpoint.

Since the conical log spiral was loaded with powdered ferrite, as reported in the final report on the previous contract covering this study (Lyon et al, 1965), it was decided to ascertain how loading of a conical log spiral with solid ferrite material would affect its frequencies of operation. The difficulties of loading with solid ferrite are that the available ferrite, EAF-2, is available only in the large bars, 7"x1"x 1/2" . Since the material cannot be readily duplicated without some expense, there has been some reluctance to machine these bars to fit any particular geometry desired at the moment. Therefore, the uncut bars were taped to the inside of the conical helix in the best way possible, leaving a minimum air gap

between the bars and the windings of the helix. The conical helix selected for this study was No. 200, the characteristics of which were detailed by Lyon et al (1965). A photograph of No. 200, loaded, is shown in Fig. 1. The lowest operating frequency of this conical helix when unloaded is approximately 360 MHz. Figures 2 and 3 show the input impedance due to a partial and full loading of the bars. Figure 2 shows the effects when bars cover only the bottom half of the conical helix and Fig. 3 shows the effects for loading over the entire interior. In each case, the bars are loaded only one bar deep, i. e. the loading was approximately a one-half inch shell. It is apparent from the figures that even at frequencies down to 280 MHz (partial loading) or 245 MHz (full loading) a VSWR of approximately 3 or less is maintained. The results indicate that the reduction in the lower operating frequency of 80 - 100 MHz may be achievable with solid bar loading, if radiation patterns also show this reduction. The results further indicate that the ferrite bars, even though they have much greater μ and ϵ than the powdered form, do not appear to cause a greater decrease in the lowest operating frequency of the conical helix than the powder causes. Further studies of impedance are planned.

The antenna patterns of this loaded conical helix were less satisfactory than the impedance behavior. The beamwidths were greater and the patterns fragmented. The presence of discrete ferrite bars may hopelessly complicate ferrite-air boundary effects. The higher μ and ϵ may emphasize such boundary effects. Further tests using much smaller strips of the Q-3 ferrite may allow a more uniform solid ferrite loading, within the acceptable frange of frequency (below 200 MHz) for this material.

2.2 Ferrite-Loaded Helical Antennas

The experimental study of the conical log spiral is being preceded by a series of experimental efforts on ferrite-loaded helical antennas, since the basis for analysis for the conical log spiral antenna is that each active region behaves approximately as an equivalent bifilar helical antenna with the same pitch angle

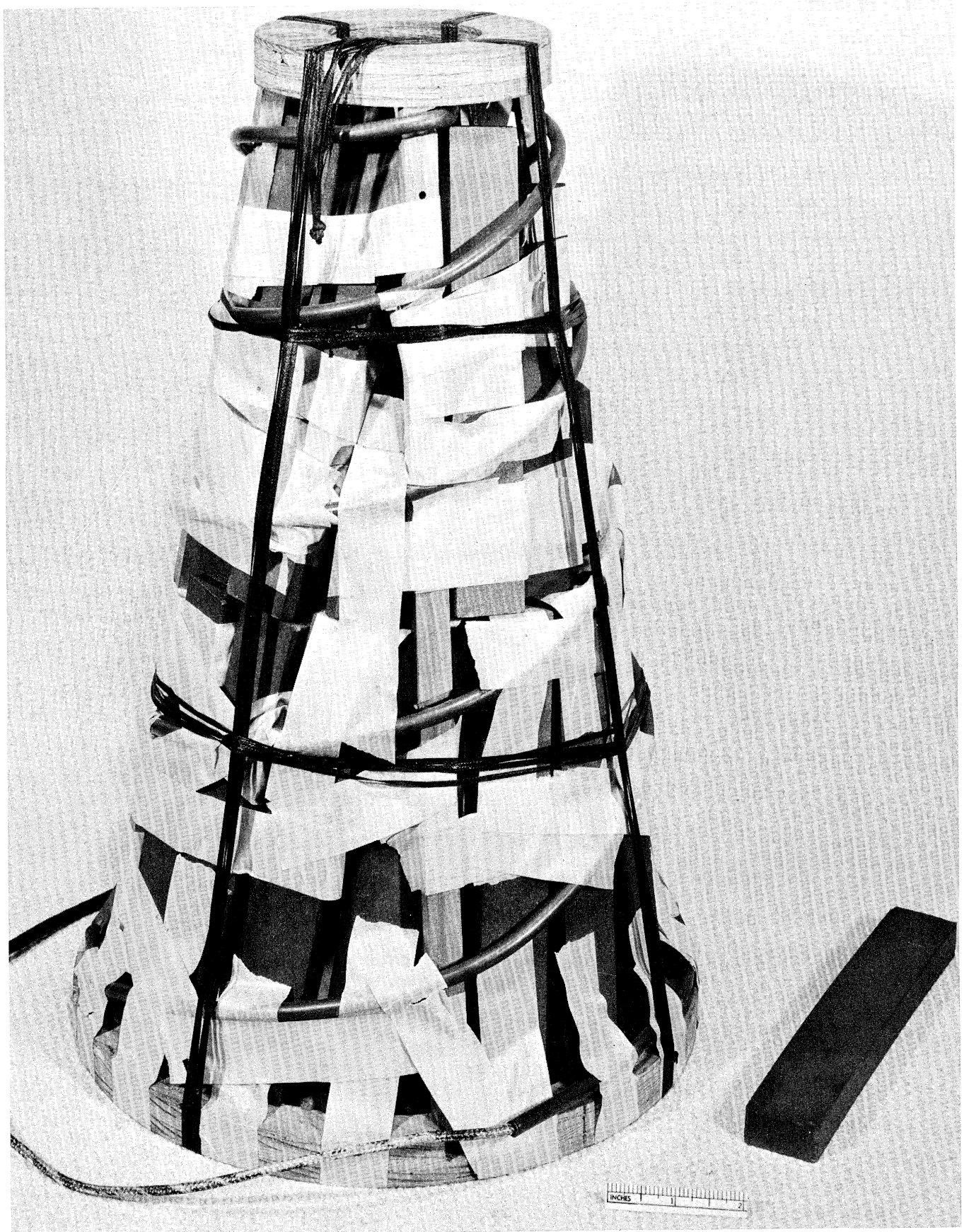


FIG. 1: CONICAL SPIRAL (No. 200) LOADED WITH SOLID FERRITE BARS

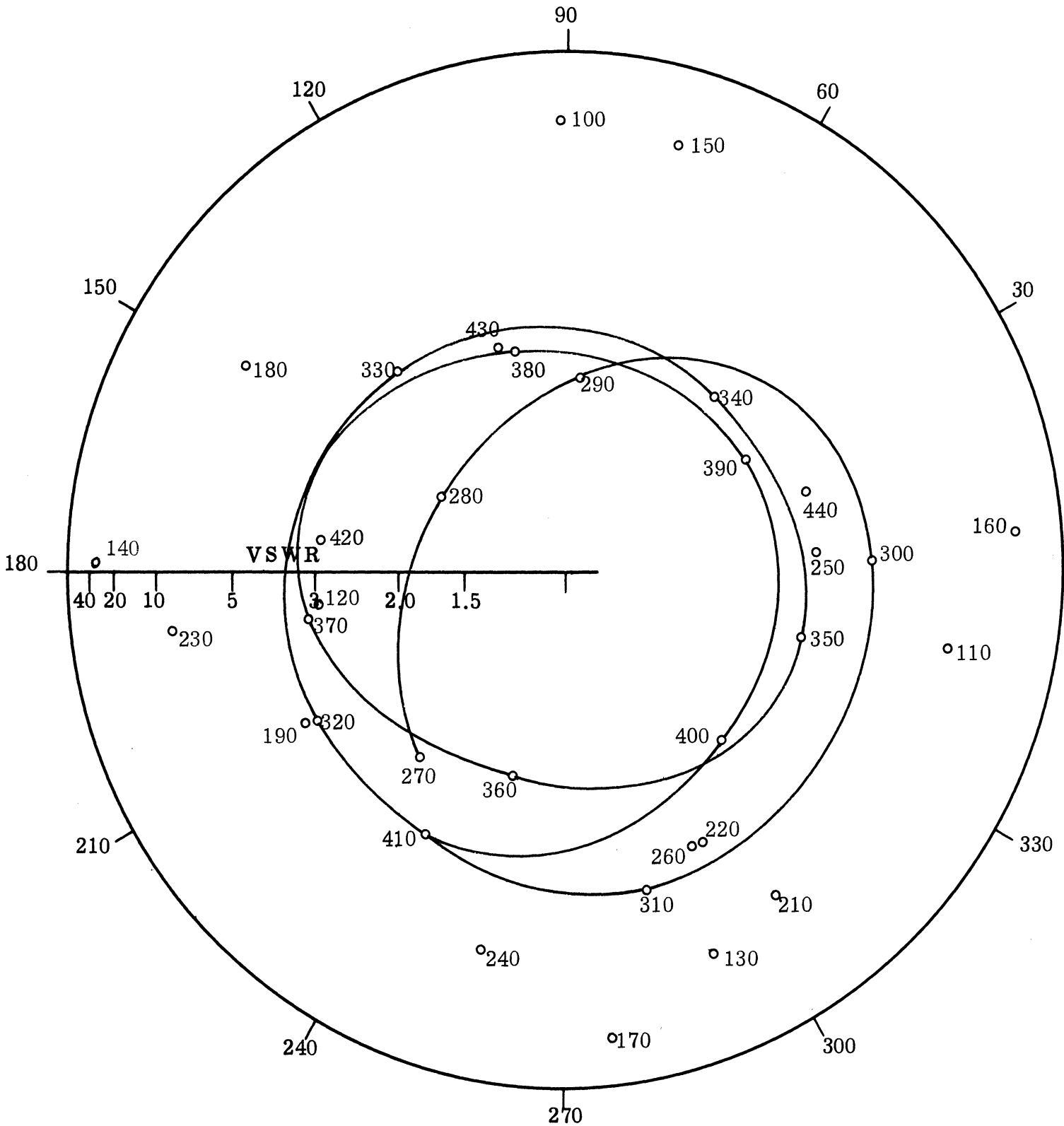


FIG. 3: IMPEDANCE DIAGRAM OF SOLID FERRITE LOADED CONICAL HELIX ANTENNA. Entire Conical Shell Loading. (Frequency MHz).

and diameter. Several turns of the log conical spiral actively participate in the radiation phenomena. It is assumed that the analysis of the loaded helix will apply at least as a preliminary step in the analysis of the log conical spiral loaded with ferrite. In the last final report (Lyon et al, 1965) there was a section on the ferrite loaded helix in which a brief analysis was made. Also, there were some simple radiation patterns given and a description of the relevance of the $K - \beta$ diagram for the unloaded helix. In recent work, considerable effort is being made to extend the interpretation of the $K - \beta$ diagram with the objective of finding more precisely the dependence of the propagation constant of the phase velocity around the turn upon the ferrite loading.

A series of experiments have been designed for various types of helical antennas. Monofilar and bifilar antennas with various diameters and pitches are used in these experiments. A number of the most informative situations are depicted in the descriptions of the experimental effort which follow.

2.2.1 Bifilar Helical Antennas.

A 4" dia. bifilar helical antenna was tested with various loadings of EAF-2 ferrite powder. The parameters of the basic antenna are listed in Table I. Figure 4 shows the basic antenna and the balsa wood insert used for retaining ferrite layers. The bifilar antenna was fed with an infinite balun set-up similar to that used in conical log spiral antennas. The validity of using this balun was partially checked by observing variations in antenna pattern as the coaxial feed was manipulated. Less than twenty percent variation in signal amplitude was noted due to such changes, indicating that antenna currents had decayed sufficiently by the end of the helix to justify using an infinite balun feed arrangement. The form upon which the helix was wound was fiberglass (Fig. 5). The effect of the fiberglass and balsa wood is presently being studied. In general the effect is expected to remain constant for the 'with' and 'without' loading cases.

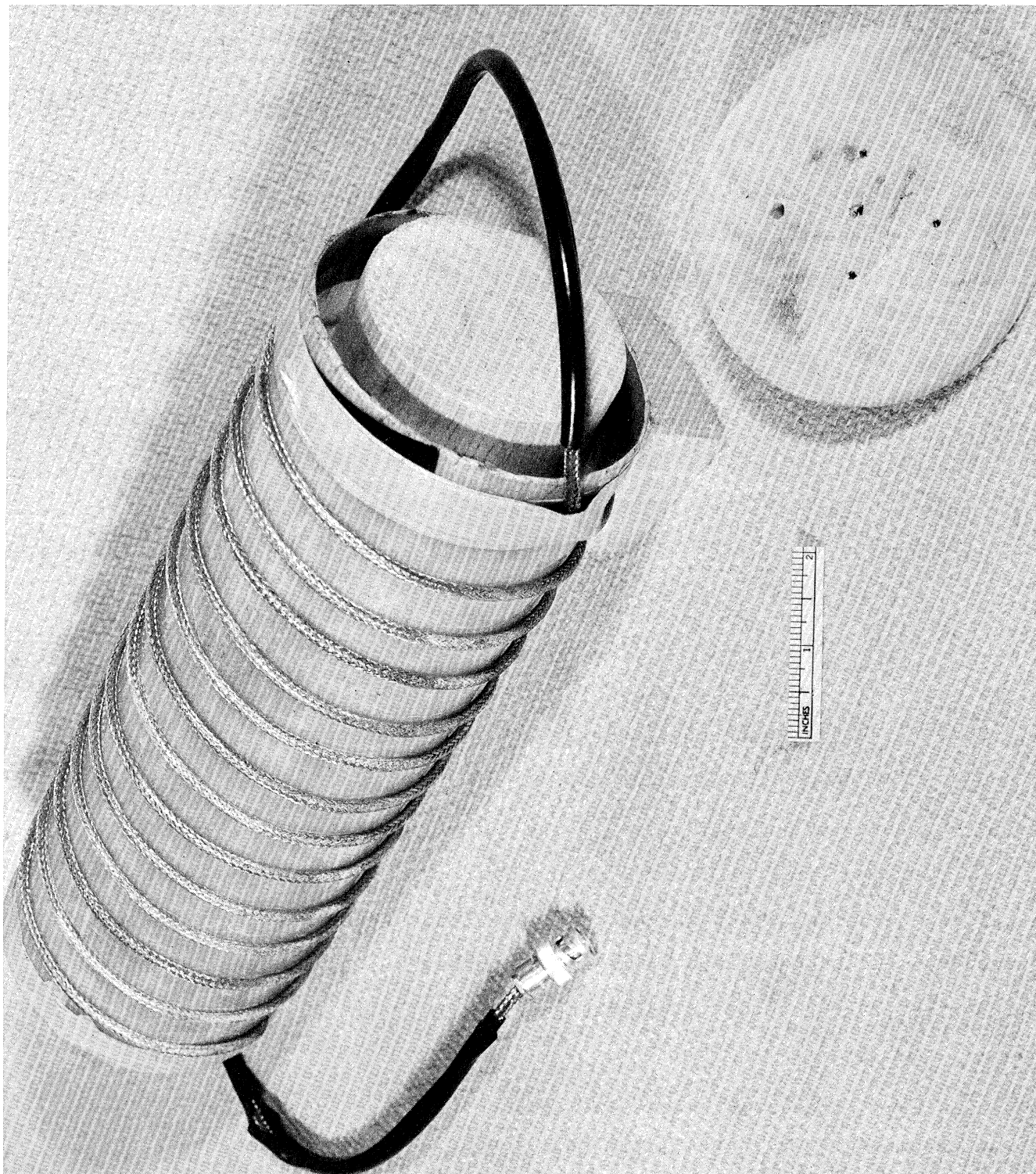


FIG. 4: BIFILAR 4" DIA. HELIX WITH BALSAM WOOD CORE AND CAP.

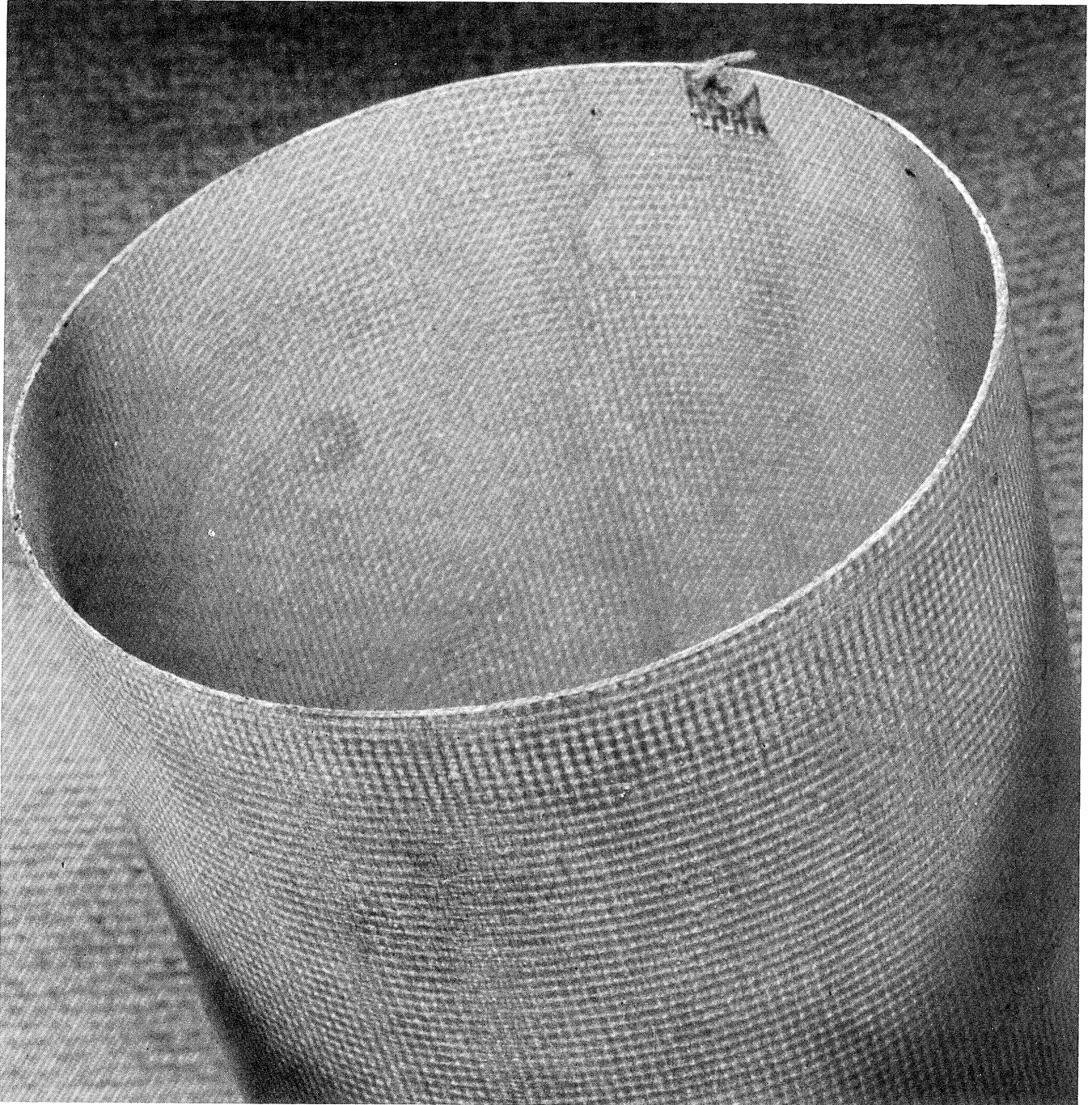


FIG. 5: FIBERGLASS-EPOXY TUBE FORM FOR HELICES.

TABLE I: ANTENNA NO. 213

| | |
|----------------|---|
| Helix Diameter | 4.15" |
| Helix Length | 10" (6.5 turns) |
| Feed Type | Infinite balun, bifilar, no ground plane. |
| Pitch | 1.5" (6.6° pitch angle). |
| Conductor | RG58U cable stripped of outer insulation. |
| Form | Fiberglass-epoxy tube, three layers (~1/16" thick, 11" long). |

In measuring antenna performance, patterns were first taken without material loading and then the core inside the helix was entirely loaded with ferrite powder as shown in Fig. 6. Patterns were taken on this antenna to observe the frequency of axial radiation and the change of this frequency with loading. Finally, the loading was reduced to an interior layer or shell by placing an insert of balsa wood, assumed to be essentially equivalent to an air core, inside the helix and placing ferrite powder between this insert and the fiberglass retaining tube (Figs. 7 and 8). One shell loading shown is with a powder 'cap' or layer at each end of the antenna; the other shell loading was without this cap.

The E_{θ} patterns of the 4" bifilar helical antenna are shown in Fig. 9 and the E_{ϕ} patterns are given in Fig. 10. Results are given for various frequencies and both the ferrite-loaded and the unloaded axial patterns are displayed. The solid patterns are for the unloaded cases, the dashed patterns are for the 1/2" powdered ferrite layer and the dotted patterns are for the ferrite powder in the entire core. The figures show that the unloaded helical antenna had an axial mode frequency at approximately 710 - 720 MHz whereas the loaded antenna, both with the full core loading and with the 1/2" layer loading, show an axial mode frequency approximately 550 - 600 MHz. Therefore, the powder loading causes a reduction of approximately 110 - 160 MHz in operating frequency.

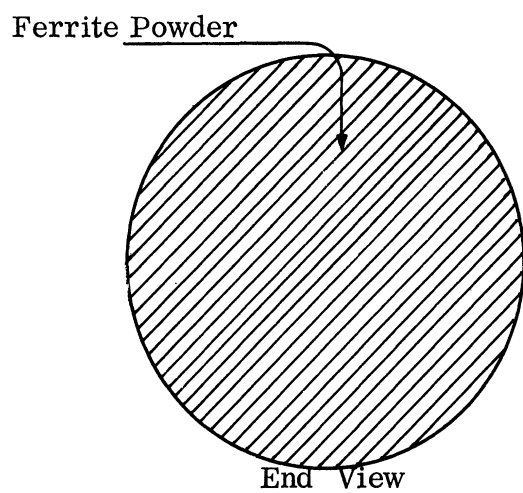
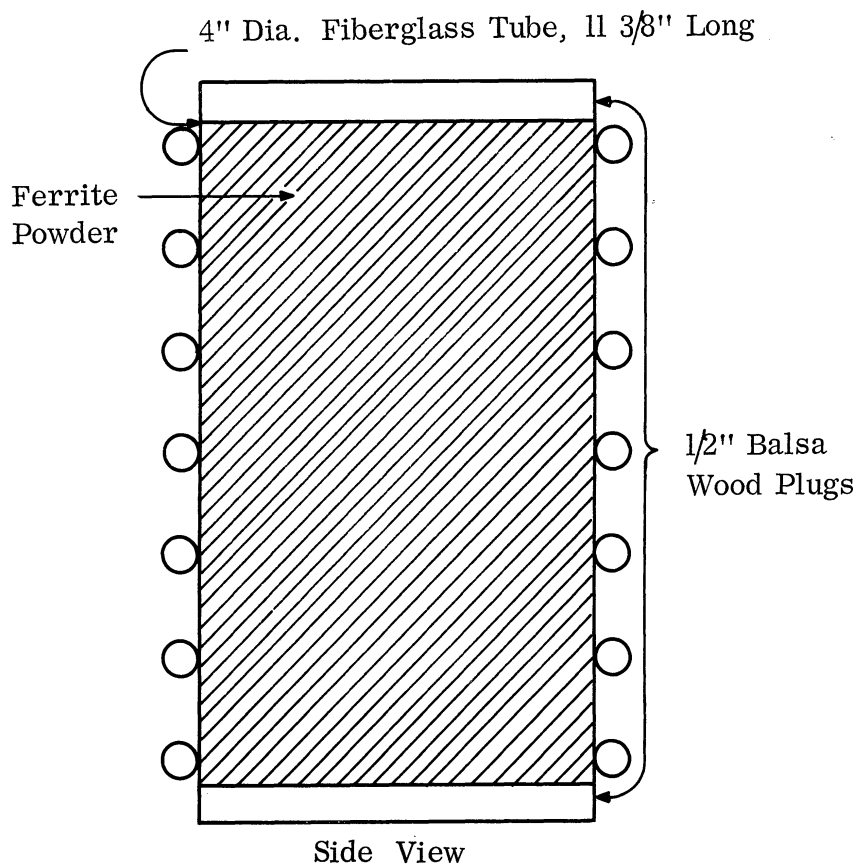


FIG. 6: LOADING DIAGRAM; BIFILAR HELIX (No. 213)
FULL CORE LOADING.

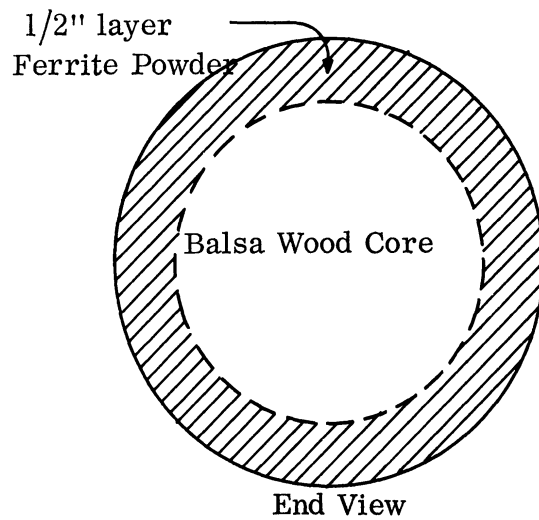
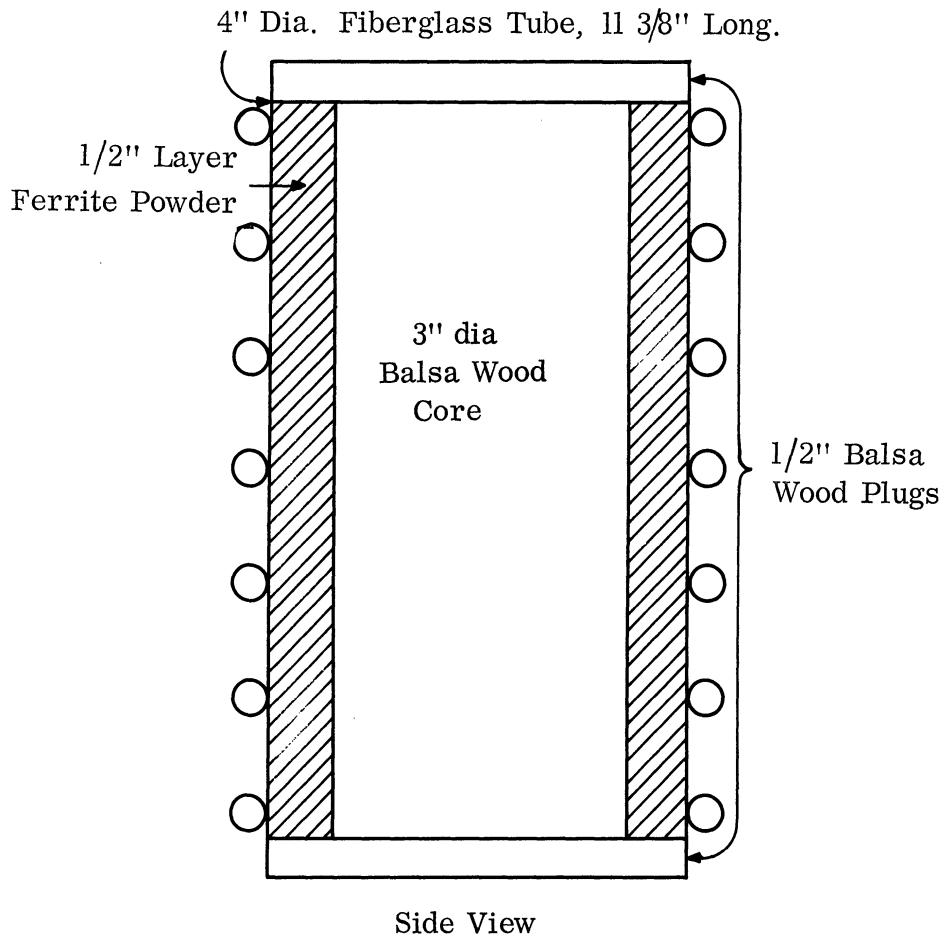


FIG. 7: LOADING DIAGRAM: BIFILAR HELIX (No. 213)
LAYER LOADING.

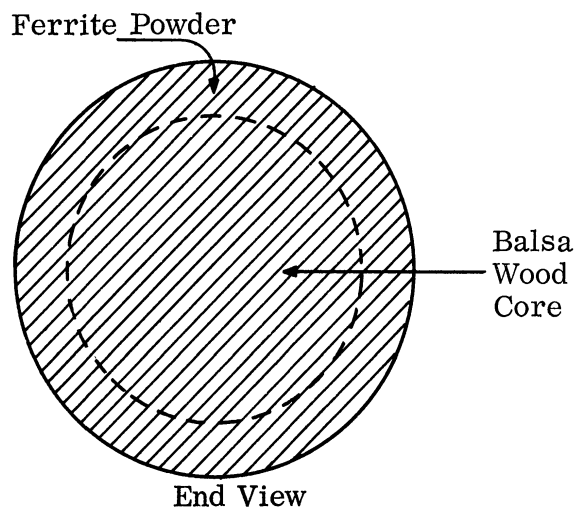
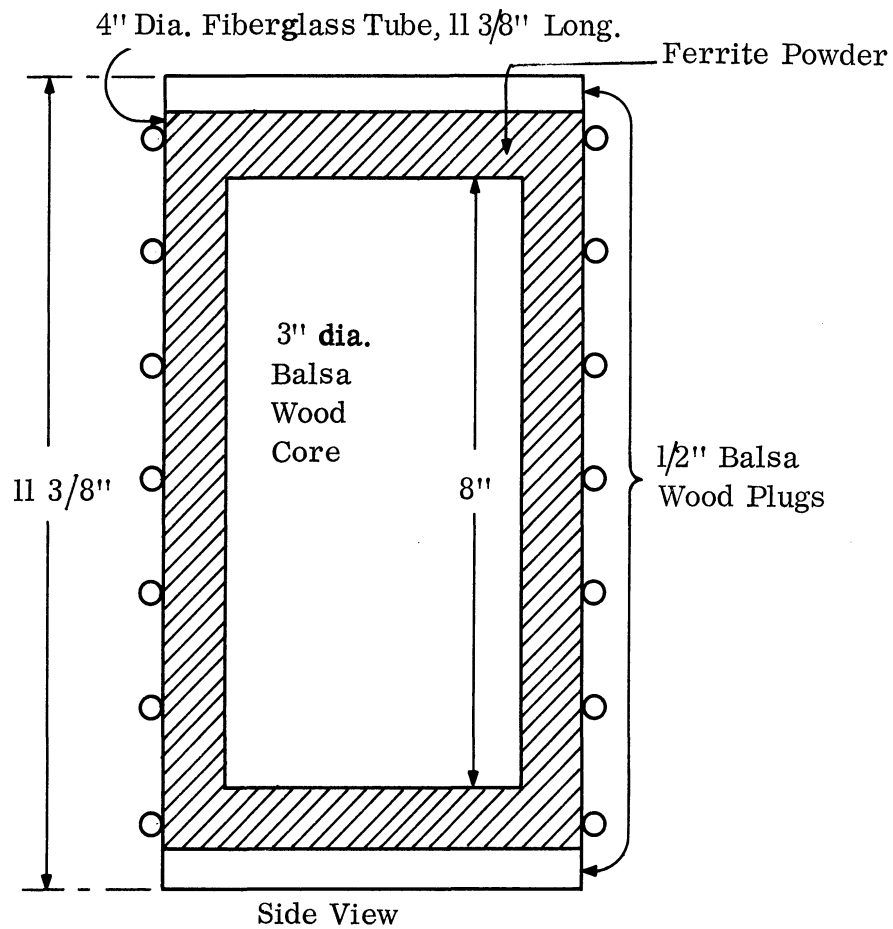


FIG. 8: LOADING DIAGRAM; BIFILAR HELIX (No. 213) LAYER
 LOADING PLUS END CAP (Ferrite Powder Thickness:
 Ends 1 3/16", Side 1/2").

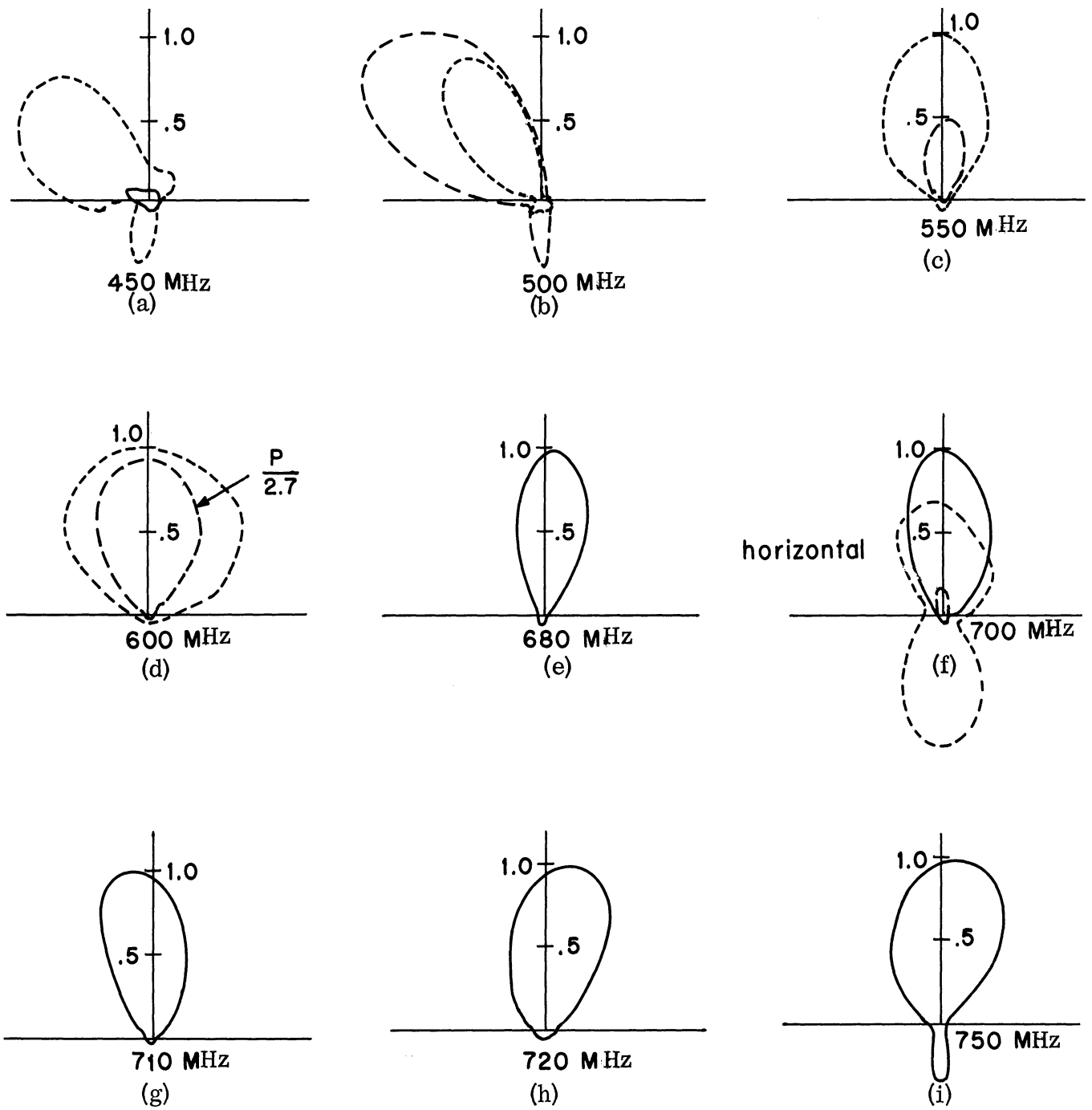


FIG. 9: BIFILAR HELIX (No. 213) ANTENNA PATTERNS. LOADED VS UNLOADED.
 E_{θ}^2 = LINEAR POWER. θ = POLAR ANGLE, P = POWER RECEIVED,
 — AIR LOADED, ---- FULL CORE FERRITE POWDER LOADING,
 - - - .5" INTERIOR LAYER FERRITE POWDER LOADING.

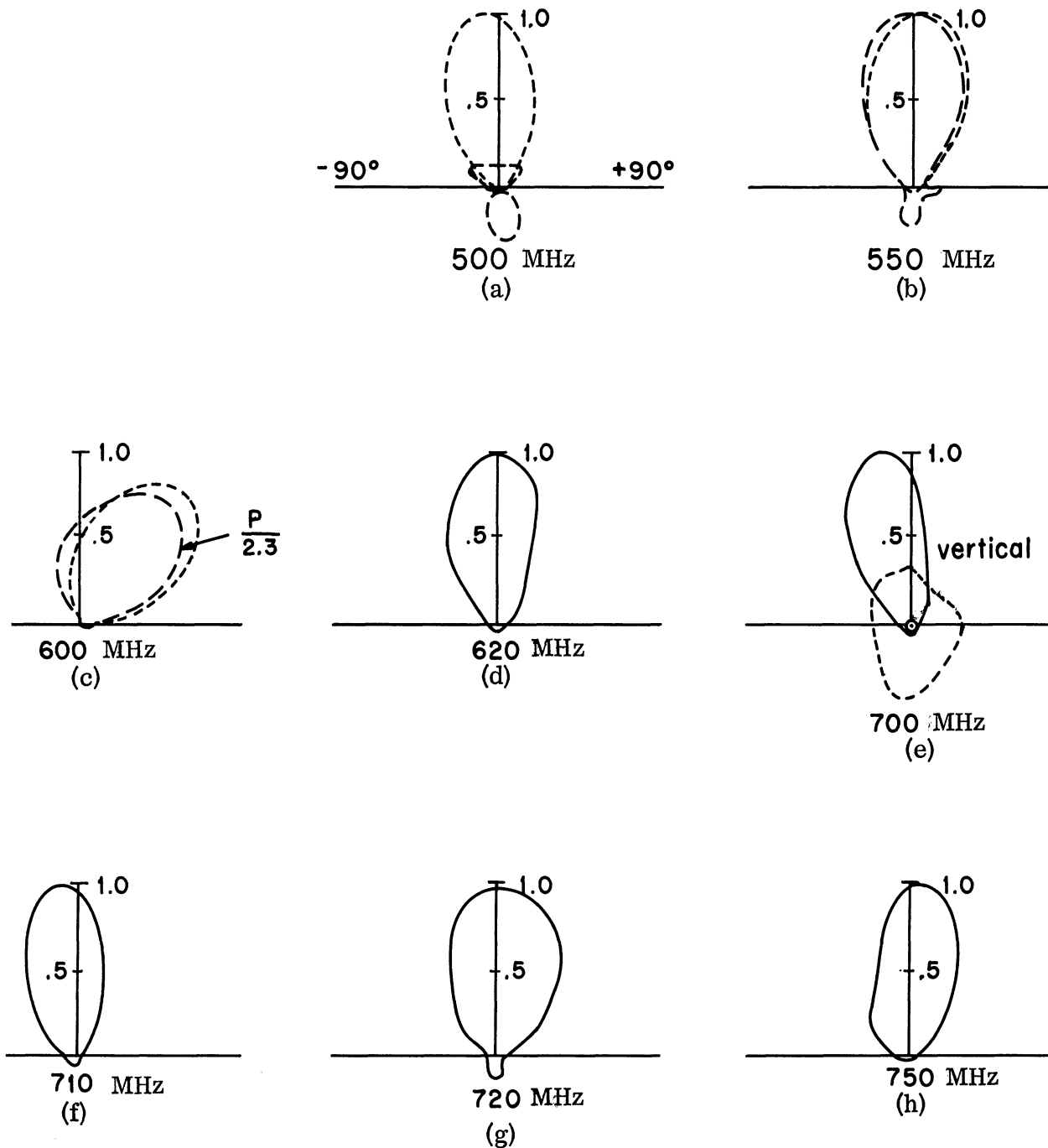


FIG. 10: BIFILAR HELIX (No. 213) ANTENNA PATTERNS. UNLOADED VS LOADED
 E_{θ}^2 = LINEAR POWER, θ = POLAR ANGLE, P = POWER RECEIVED,
 — AIR LOADED, ---- FULL CORE FERRITE POWDER LOADED,
 - - - .5" INTERIOR LAYER FERRITE POWDER LOADED

It should be noted that relative amplitudes between different frequencies or polarizations are not comparable due to normalizations made in drawing the patterns. The only relative amplitudes that are comparable are those appearing on one sub-plot, i. e. the same frequency and polarization. These comparisons within sub-plots were plotted relative to a constant matched power in and therefore indicate relative radiation efficiency.

There are certain discrepancies in Figs. 9 and 10. For example, at 600 MHz, one polarization shows an on-axis pattern and the other polarization shows an off-axis pattern. Furthermore, at 500 MHz, one polarization indicates that full core loading has a larger amplitude, whereas the other indicates a larger amplitude from the partial core or shell loading. Even though amplitudes between plots are not comparable, one expects a conclusion as to the best loading method to be the same for both polarizations of a circularly polarized antenna. This anomaly in results is probably due to pattern asymmetry, indicated by a measured axial ratio of approximately 1.3 in both loaded antennas. Also, at 500 MHz, one polarization indicates that full core loading is more effective, whereas the other polarization indicates that neither loading is very effective due to an off-axis main lobe. It is apparent that more comparison data is necessary for air core helical antenna. Such anomalies of data will be removed or clarified in the final report.

2.2.2 Monofilar Helices

In order to determine the effects of ferrite powdered loading on monofilar helices, several tests of 4" and 5" dia. helices were fabricated. The specifications for Antenna No. 215 (Fig. 11) are given in Table II and antenna patterns are presented in Figs. 12 and 13.

Several conclusions may be drawn from these figures. First, a reduction of the center operating frequency due to loading, of about 150 MHz, (approx. 650 MHz to 500 MHz) is seen. Second, the radiated powers for the ferrite loaded case are

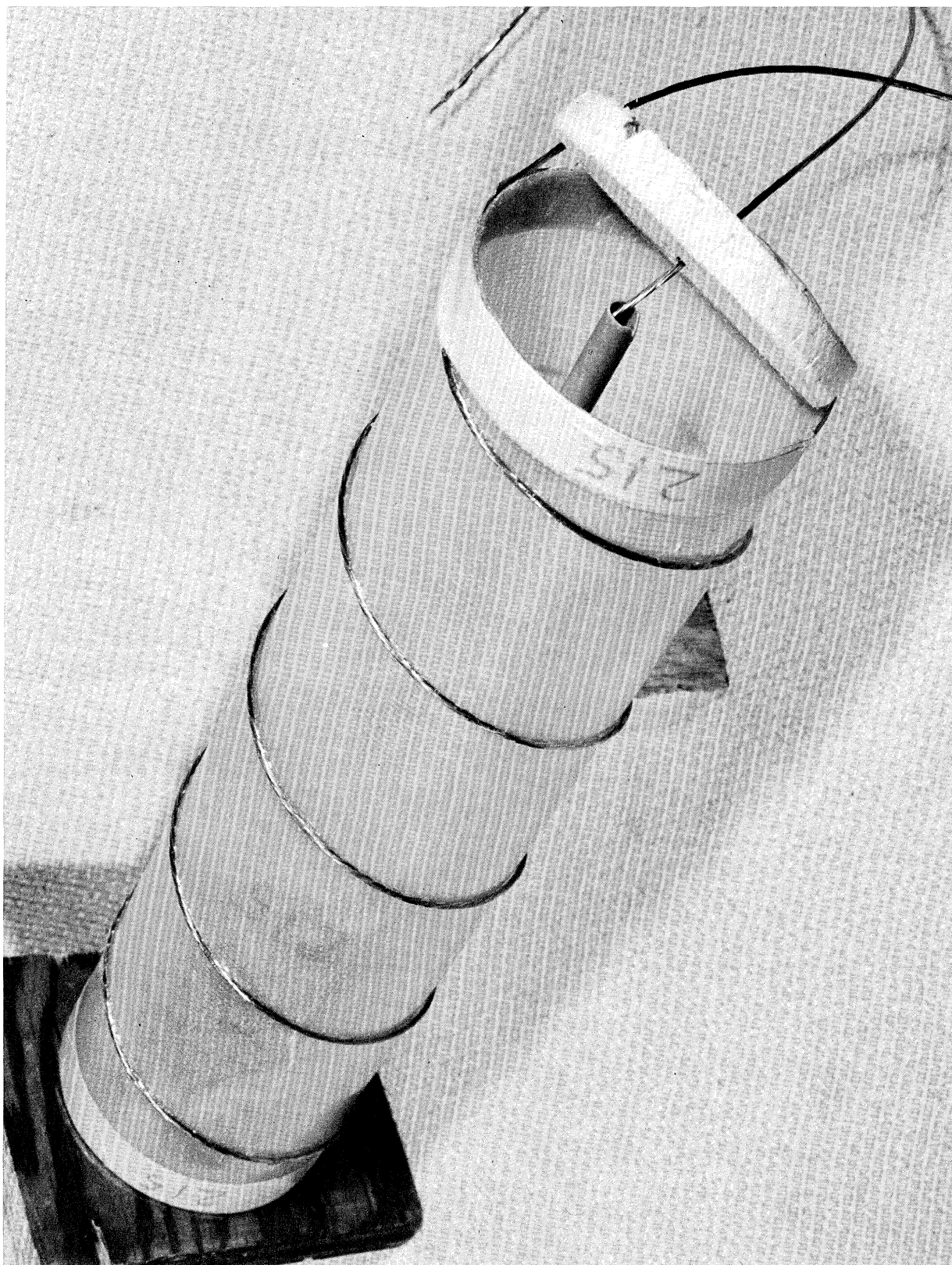


FIG 11: MONOFILAR 4" HELIX WITH SMALL TUBE FOR CENTER CONDUCTOR.

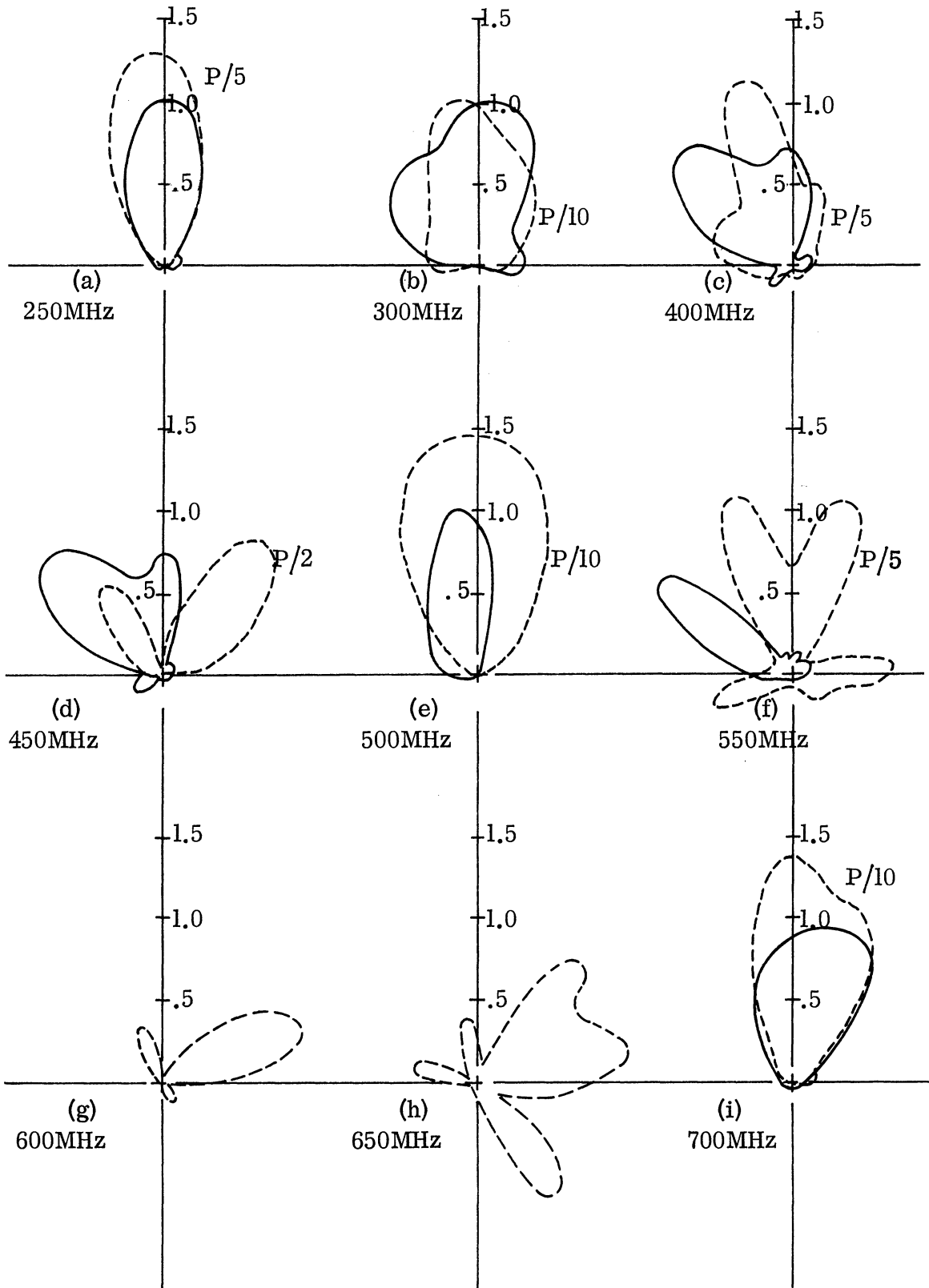


FIG. 12: 4" DIA. MONOFILAR HELIX (NO. 215) $|E_\theta|^2$ LINEAR POWER.
 — UNLOADED, --- FULL CORE FERRITE POWDER LOADED.
 P = POWER RECEIVED.

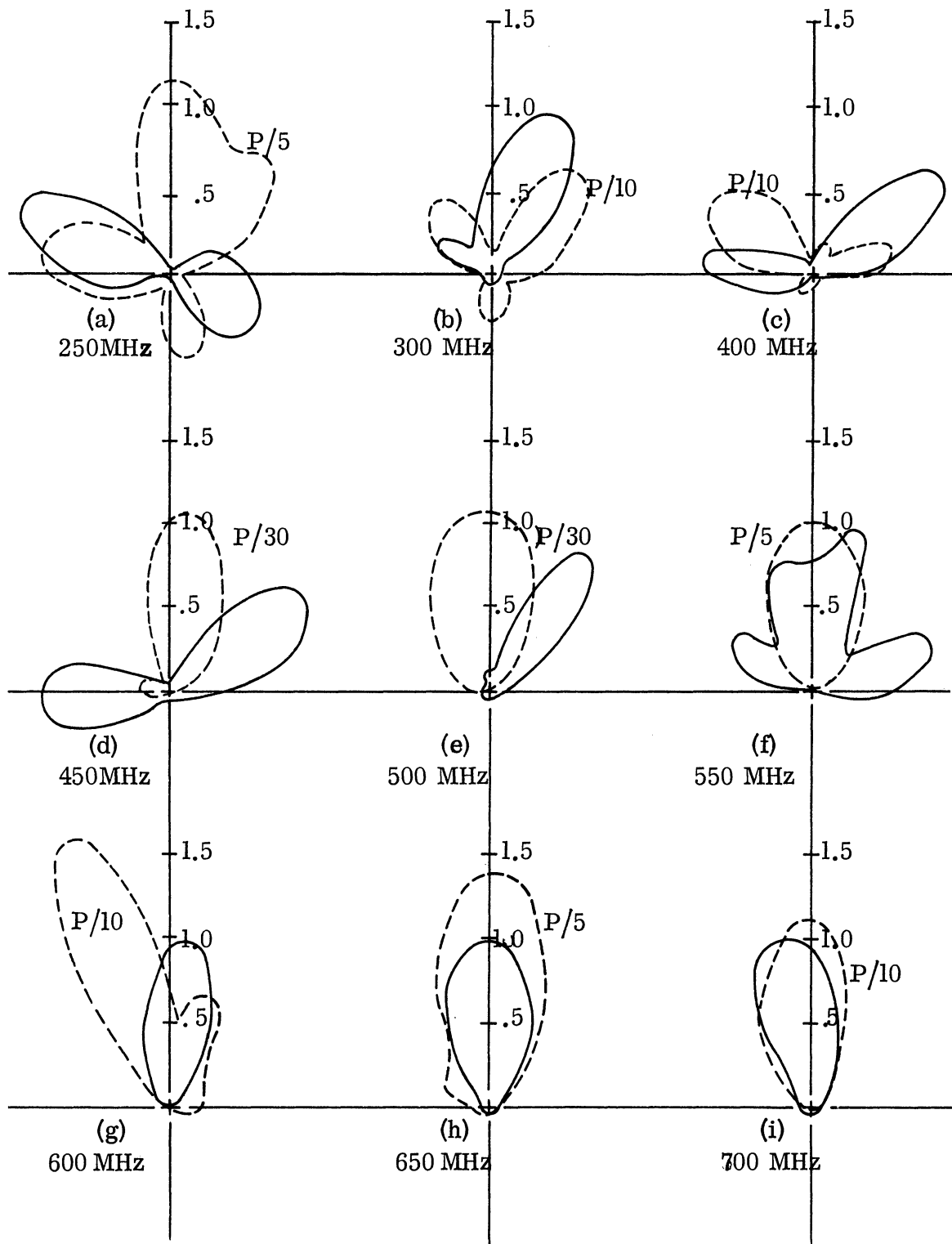


FIG. 13: 4" DIA. MONOFILAR HELIX (NO. 215) $|E_{\theta}|^2$ LINEAR POWER .
 — UNLOADED --- FULL CORE FERRITE POWDER LOADED.
 P = POWER RECEIVED.

much greater than for the air loaded case (the notation P/N, referring to the ferrite case on the figures, indicates that the power received divided by N was plotted). Since the plots are relative to a constant net (matched) power input, the greater received power is apparently due to increased radiation efficiency. This result will be re-checked.

TABLE II: ANTENNA NO. 213

| | |
|----------------|---|
| Helix Diameter | 4" |
| Helix Length | 5 turns |
| Pitch | 3" (13° pitch angle) |
| Conductor | 7 strand, 14 guage, copper stranded antenna wire. |
| Form | Fiberglass tube, 14" long 3 layers thick (1/16") |
| Feed | Ground plane, type N connector. |

III FERRITE SLOT ARRAYS

In order to study the effects of magnetic fields on ferrite radiators, a preliminary design for an array of slots placed in a waveguide filled with ferrite material has been made. The array has not been fabricated; plans for the investigation are being worked out.

3.1 Ferrite Waveguide Preliminary Tests

The waveguide filled with ferrite is shown in Figs. 14 and 15. This waveguide will be used for preliminary tests; transmission characteristics will be measured with emphasis on insertion loss. One objective will be to find out whether the ferrite filling composed of small sticks of ferrite is adequate. There is some question as to whether the interstices associated with this assemblage of sticks offer a detrimental influence. Hopefully, the interstices effect has been minimized by aligning the long dimension of the sticks with the direction of propagation of energy in the waveguide. This preliminary experiment should serve as a check on the coupling arrangements from the coaxial cables used to feed power to the waveguide and extract power from the waveguide.

3.2 Preliminary Non-resonant Array Tests

A preliminary design of an array of several slots with an array length somewhat over three wavelengths in free space for operation in the vicinity of 200 MHz or less is shown in Fig. 16. This array has been designed so that it is a non-resonant array making use of the traveling wave from right to left in Fig. 16. Although the array has several slots, its directivity will be quite low since this depends on the array length in air. Each of the slots of the array is filled with ferrite material; otherwise, these slots would be below cut-off frequency. This array can be modified by having an additional $1/8$ " layer of ferrite caused by having one stick of ferrite placed on top of the ferrite in the slot. The slots have been designed

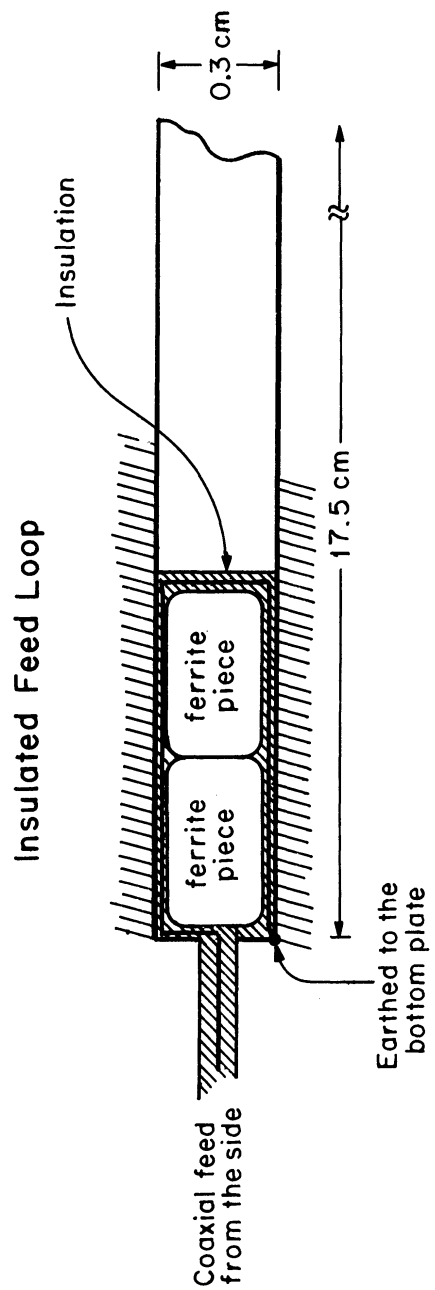
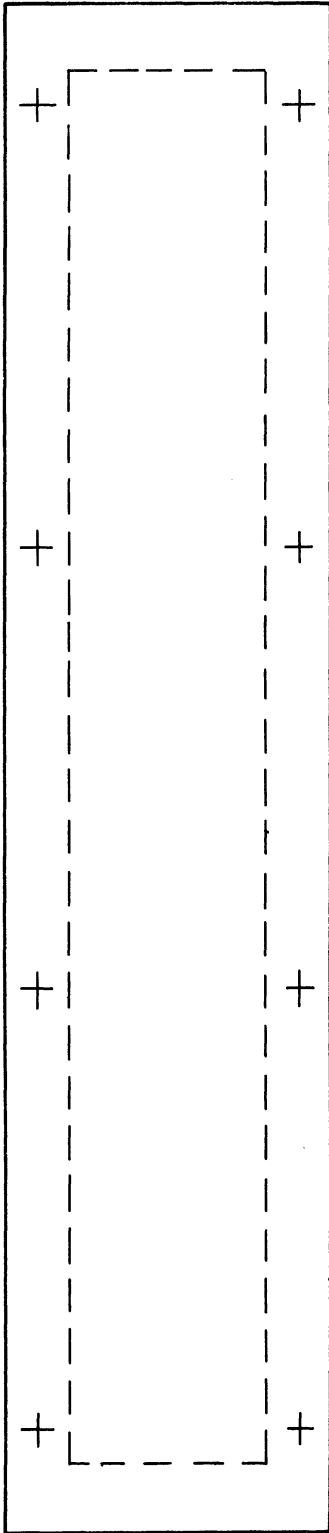
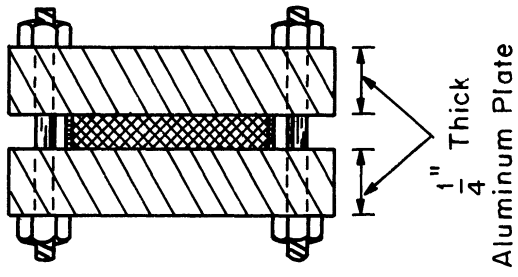


FIG. 14: PROPOSED MECHANICAL CONFIGURATION FOR WAVEGUIDE TEST.

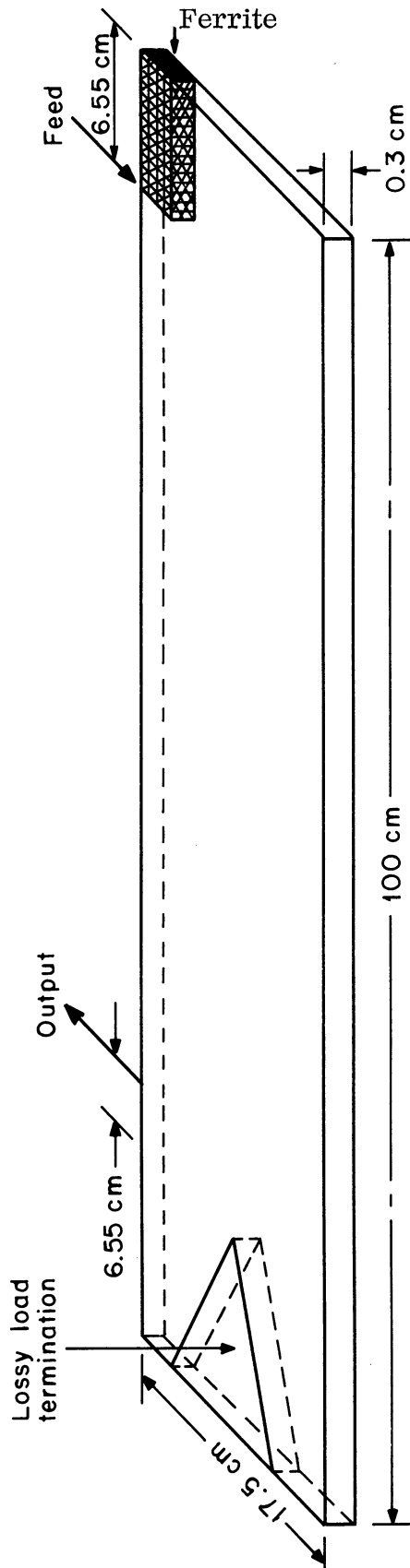


FIG. 15: EXPERIMENTAL DETAILS TO DETERMINE INSERTION LOSS OF WAVEGUIDE.
Thickness of one ferrite strip = 0.3cm. Dimensions of one ferrite piece=2.82"x0.49"x0.12".
Fourteen pieces lengthwise = 100cm. 14 pieces width-wise = 17.5cm.

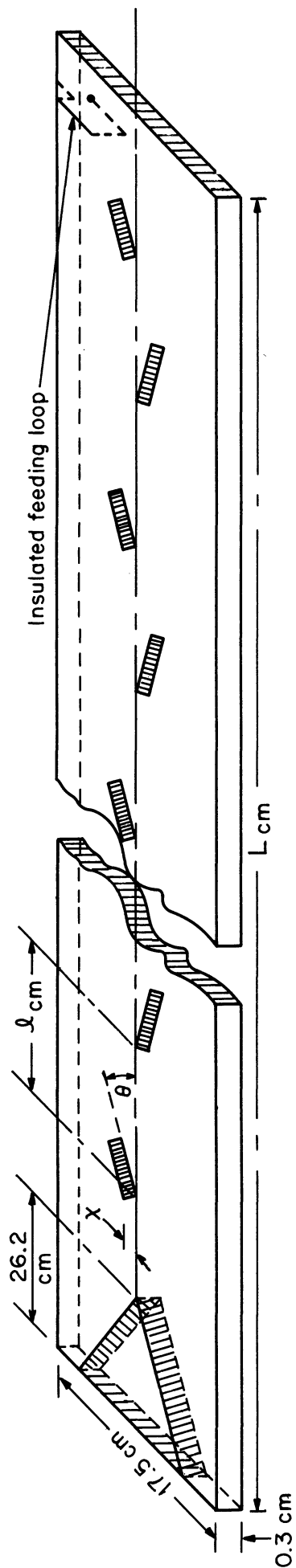


FIG. 16: SIMPLIFIED DIAGRAM OF 9-SLOT FERRITE LOADED WAVEGUIDE ARRAY

with a dimension of 0.5"x2.83"x0.125". The ferrite to be used in this design is Q-3, manufactured by Indiana General Corporation. This ferrite is relatively new to this project; more information on the material is given in Section IV.

3.3 Magnetic Bias Control of Ferrite Array

The array shown in Fig. 16 has been designed to demonstrate the usefulness of ferrites in such an antenna. The use of ferrite material offers a possible method for controlling beam shape or position by the application of a magnetic field. For the purpose of demonstrating magnetic control, a still simpler array is contemplated. For this purpose an array having only three slots may be used. The space between adjacent slots will be such that a magnetic field can readily be produced by pole faces placed in these regions. The most convenient arrangement for pole pieces is to have a magnetic field which will line up with the direction of the E-field in the waveguide. The application of a magnetic field in this direction offers the possibility of control by causing a phase shift in the transmission mode between each two slots. For the 3-slot array, there are two such intervals for the application of magnetic field. At each of these two locations, the extent of the magnetic pole piece in the direction of propagation would be important. It is through the active width of the magnetic field pole piece that the permeability of the ferrite can be changed (reduced). An important advantage of this simple design is that it allows the magnetic pole pieces to be very close together. In previous experiments on the magnetic control of slot radiators, the distance between the pole pieces was much greater. The arrangement discussed here should make possible the use of magnetic fields greatly in excess of those previously used; fields as high as 1500 Gauss may be obtained.

IV

ENERGY TRANSFER TO FERRITE SLAB

Studies have been made of continuously excited (i. e. excited over a large portion of the antenna length) traveling wave antennas (Spitz, 1962; Walter, 1965; Weeks, 1957; Rumsey, 1953). Recently, this laboratory began studies of such antennas using ferrite materials. Specifically, a mathematical study of the energy transfer process from the exciter (in our case, a helix) to the ferrite slab (the intended radiating mechanism) has been made.

In a study of energy transfer into a ferrite slab one can start with the proposition that with two transmission lines coupled together, energy fed into one line will be transferred optimally to the second, under certain conditions. The voltage and current differential equations for each of the two transmission lines have been written. A consideration of the coefficients involved in these transmission lines indicates the dependence upon mutual coupling factors. When the second transmission line is to serve as a radiator, it is expected that the energy transferred to this line will be radiated at the far end in the end fire direction.

4.1 Analysis

In order to cause a strong coupling between the feeding electric circuit and the receiving ferrite slab the phase velocity of the electric circuit in the axial direction must be adjusted to be approximately the same as the wave phase velocity in the ferrite slab.

The phase velocity of the helix of the electric circuit is approximately:

$$v_p = c \sin \psi$$

where ψ is the pitch angle and c is the velocity of light. Treating the helix as a transmission line with distributed L and C , the ferrite slab may be considered to be another transmission line. The arrangement of lines is shown in Fig. 17. Due to

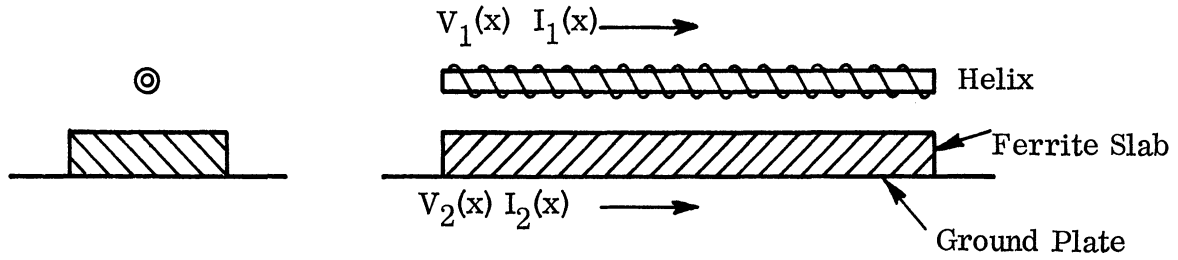


FIG. 17: COUPLED FERRITE SLAB ANTENNA

the excitation of the helix, there is mutual coupling between the helix and the ferrite slab. The circuit equations are

Circuit No. 1: Helix:

$$\left\{ \begin{array}{l} \frac{dV_1}{dx} = z_1 I_1 + z_{12} I_2 \end{array} \right. \quad (1)$$

$$\left\{ \begin{array}{l} \frac{dI_1}{dx} = y_1 V_1 + y_{12} V_2 \end{array} \right. \quad (2)$$

Circuit No. 2: Ferrite

$$\left\{ \begin{array}{l} \frac{dV_2}{dx} = z_2 I_2 + z_{21} I_1 \end{array} \right. \quad (3)$$

$$\left\{ \begin{array}{l} \frac{dI_2}{dx} = y_2 V_2 + y_{21} V_1 \end{array} \right. \quad (4)$$

Let

$$Z_1 = \sqrt{z_1/y_1}, \quad Z_2 = \sqrt{z_2/y_2} \quad (5)$$

Multiply equation (2) by $\pm Z_1$ and add the result to (1),

$$\frac{d}{dx} (V_1 \pm I_1 Z_1) = \pm \sqrt{z_1 y_1} (V_1 \pm I_1 Z_1) + z_{12} I_2 \pm y_{12} Z_1 V_2 \quad (6)$$

Multiply (4) by $\pm Z_2$ and add the result to (3),

$$\frac{d}{dx} (V_2 \pm I_2 Z_2) = \pm \sqrt{z_2 y_2} (V_2 \pm I_2 Z_2) + z_{21} I_1 \pm y_{21} Z_2 V_1 \quad (7)$$

Define the following modes.

$$A_{1\pm} = \frac{V_1 \pm I_1 Z_1}{4\sqrt{Z_1}}, \quad A_{2\pm} = \frac{V_2 \pm I_2 Z_2}{4\sqrt{Z_2}} \quad (8)$$

There are two modes (+ = forward, - = backward waves) propagating in each circuit. All modes mentioned are a subclassification within the TEM mode existing on each line.

$$\begin{cases} V_1 = 2\sqrt{Z_1}(A_{1+} + A_{1-}) \\ I_1 = \frac{2}{\sqrt{Z_1}}(A_{1+} - A_{1-}) \end{cases} \quad \text{for Circuit No. 1} \quad (9)$$

$$\begin{cases} V_2 = 2\sqrt{Z_2}(A_{2+} + A_{2-}) \\ I_2 = \frac{2}{\sqrt{Z_2}}(A_{2+} - A_{2-}) \end{cases} \quad \text{for Circuit No. 2} \quad (10)$$

Substituting (8), (9) and (10) into (6) and (7) yields

$$\begin{cases} \left(\frac{d}{dx} + \sqrt{z_1 y_1}\right)A_{1\pm} = \frac{z_{12}}{2\sqrt{Z_1 Z_2}}(A_{2+} - A_{2-}) \pm \frac{y_{12}\sqrt{Z_1 Z_2}}{2}(A_{2+} + A_{2-}) \\ \left(\frac{d}{dx} + \sqrt{z_2 y_2}\right)A_{2\pm} = \frac{z_{21}}{2\sqrt{Z_1 Z_2}}(A_{1+} - A_{1-}) \pm \frac{y_{21}\sqrt{Z_1 Z_2}}{2}(A_{1+} + A_{1-}) \end{cases} \quad (11)$$

$$\begin{cases} \left(\frac{d}{dx} + \sqrt{z_1 y_1}\right)A_{1\pm} = \frac{z_{12}}{2\sqrt{Z_1 Z_2}}(A_{2+} - A_{2-}) \pm \frac{y_{12}\sqrt{Z_1 Z_2}}{2}(A_{2+} + A_{2-}) \\ \left(\frac{d}{dx} + \sqrt{z_2 y_2}\right)A_{2\pm} = \frac{z_{21}}{2\sqrt{Z_1 Z_2}}(A_{1+} - A_{1-}) \pm \frac{y_{21}\sqrt{Z_1 Z_2}}{2}(A_{1+} + A_{1-}) \end{cases} \quad (12)$$

Next, equations (11) and (12) upon regrouping coefficients can be written,

$$\left(\frac{d}{dx} + \sqrt{z_1 y_1}\right)A_{1\pm} = \left(\frac{z_{12}}{2\sqrt{Z_1 Z_2}} \pm \frac{y_{12}\sqrt{Z_1 Z_2}}{2}\right)A_{2+} - \left(\frac{z_{12}}{2\sqrt{Z_1 Z_2}} \mp \frac{y_{12}\sqrt{Z_1 Z_2}}{2}\right)A_{2-} \quad (13)$$

$$\left(\frac{d}{dx} + \sqrt{z_2 y_2}\right)A_{2\pm} = \left(\frac{z_{21}}{2\sqrt{Z_1 Z_2}} \pm \frac{y_{21}\sqrt{Z_1 Z_2}}{2}\right)A_{1+} - \left(\frac{z_{21}}{2\sqrt{Z_1 Z_2}} \mp \frac{y_{21}\sqrt{Z_1 Z_2}}{2}\right)A_{1-} \quad (14)$$

Note that A_{1+} means $A_{1+}(x)$. This simplified notation is used from here on. The above equations of specialized forms are the more general set of equations for the coupling of physical systems in terms of modes $a_1, a_2,$ etc.

$$\frac{da_1}{dx} = c_{11}a_1 + c_{12}a_2 + c_{13}a_3 + \dots \quad (15)$$

$$\frac{da_2}{dx} = c_{21}a_1 + c_{22}a_2 + c_{23}a_3 + \dots \quad (16)$$

$$\frac{da_3}{dx} = c_{31}a_1 + c_{32}a_2 + c_{33}a_3 + \dots \quad (17)$$

Note that each of the above equations applies for each of the lines; the numerical subscript used in these is a mode designation much like the + and - used heretofore.

Now:

- A_{1+} = forward mode in Circuit No. 1
- A_{2+} = forward mode in Circuit No. 2
- A_{1-} = backward mode in Circuit No. 1
- A_{2-} = backward mode in Circuit No. 2.

From equations (11) and (12) there are four possibilities of coupling among these four modes and these are

- (1) coupling between A_{1+} and A_{2+}
- (2) coupling between A_{1+} and A_{2-}
- (3) coupling between A_{1-} and A_{2+}
- (4) coupling between A_{1-} and A_{2-}

The total or net power of the two lines at any plane located a distance x from the origin is given by

$$P(x) = \text{Re} \frac{V_1(x)I_1^*(x)}{2} + \text{Re} \frac{V_2(x)I_2^*(x)}{2} \quad (18)$$

Expressing P in terms of modes, this becomes

$$P(x) = 2 \left[|A_{1+}(x)|^2 - |A_{1-}(x)|^2 + |A_{2+}(x)|^2 - |A_{2-}(x)|^2 \right] \quad (19)$$

Evaluating P at $x = 0$ yields

$$P(0) = 2 \left[|A_{1+}(0)|^2 - |A_{1-}(0)|^2 \right] \quad (20)$$

Consider each of the four possibilities or cases of coupling in turn.

Coupling between two forward modes A_{1+} and A_{2+}

$$\left(\frac{d}{dx} - \sqrt{z_1 y_1} \right) A_{1+} = \left(\frac{z_{12}}{2\sqrt{z_1 z_2}} + \frac{y_{12}\sqrt{z_1 z_2}}{2} \right) A_{2+} - \left(\frac{z_{12}}{2\sqrt{z_1 z_2}} - \frac{y_{12}\sqrt{z_1 z_2}}{2} \right) A_{2-} \quad (21)$$

$$\left(\frac{d}{dx} - \sqrt{z_2 y_2} \right) A_{2+} = \left(\frac{z_{21}}{2\sqrt{z_1 z_2}} + \frac{y_{21}\sqrt{z_1 z_2}}{2} \right) A_{1+} - \left(\frac{z_{21}}{2\sqrt{z_1 z_2}} - \frac{y_{21}\sqrt{z_1 z_2}}{2} \right) A_{1-} \quad (22)$$

If the following inequality holds true for the greatest power transfer from Line No. 1 to Line 2,

$$\left| \frac{z_{12}}{2\sqrt{z_1 z_2}} + \frac{y_{12}\sqrt{z_1 z_2}}{2} \right| \gg \left| \frac{z_{12}}{2\sqrt{z_1 z_2}} - \frac{y_{12}\sqrt{z_1 z_2}}{2} \right|$$

Then equations (21) and (22) simplify as

$$\left(\frac{d}{dx} - \sqrt{z_1 y_1} \right) A_{1+} = \left(\frac{z_{12}}{2\sqrt{z_1 z_2}} + \frac{y_{12}\sqrt{z_1 z_2}}{2} \right) A_{2+} \quad (23)$$

$$\left(\frac{d}{dx} - \sqrt{z_2 y_2} \right) A_{2+} = \left(\frac{z_{21}}{2\sqrt{z_1 z_2}} + \frac{y_{21}\sqrt{z_1 z_2}}{2} \right) A_{1+} \quad (24)$$

Using the general forms for coupling there results,

$$\left(\frac{d}{dx} + jC_{11} \right) A_1 = C_{12} A_2 \quad \text{and} \quad \left(\frac{d}{dx} + jC_{22} \right) A_2 = C_{21} A_1$$

The above equations are correct for either forward or backward waves. Assume

A_{1+} and A_{2+} vary as $e^{\gamma x}$,

$$\left\{ \begin{array}{l} (\gamma + jC_{11})A_{1+} = C_{12}A_{2+} \\ (\gamma + jC_{22})A_{2+} = C_{21}A_{1+} \end{array} \right. \quad (25)$$

$$\left\{ \begin{array}{l} (\gamma + jC_{11})A_{1+} = C_{12}A_{2+} \\ (\gamma + jC_{22})A_{2+} = C_{21}A_{1+} \end{array} \right. \quad (26)$$

For a nontrivial solution, the determinant of (25) and (26) must be zero; this yields

$$\gamma, \gamma' = -j \frac{C_{11} + C_{22}}{2} \pm \sqrt{C_{12}C_{21} - \left(\frac{C_{11} - C_{22}}{2}\right)^2} \quad (27)$$

Equations (25) and (26) are solved for a pair of values γ and γ' which apply only for coupling between A_{1+} and A_{2+} modes

$$A_{1+}(x) = Me^{\gamma x} + Ne^{\gamma' x} \quad (28)$$

If the γ 's are imaginary, the coupling is called passive; if they are complex, the coupling is called active. Then the solution for each of the two lines must be

$$\left\{ \begin{array}{l} A_{1+}(x) = Me^{\gamma x} + Ne^{\gamma' x} \\ A_{2+}(x) = \frac{1}{C_{12}} \left[\frac{dA_{1+}(x)}{dx} + jC_{11}A_{1+}(x) \right] \end{array} \right. \quad (29)$$

$$\left\{ \begin{array}{l} A_{1+}(x) = Me^{\gamma x} + Ne^{\gamma' x} \\ A_{2+}(x) = \frac{1}{C_{12}} \left[\frac{dA_{1+}(x)}{dx} + jC_{11}A_{1+}(x) \right] \end{array} \right. \quad (30)$$

Initial conditions are:

$$A_{1+}(x) = A_{1+}(0) \quad (31)$$

$$A_{2+}(x) = 0 \quad \text{at } x = 0 \quad (32)$$

The resulting values of the coefficients M and N are,

$$M = \frac{A_{1+}(0) [\gamma' + jC_{11}]}{j2\delta} \quad (33)$$

$$N = - \frac{A_{1+}(0) [\gamma + jC_{11}]}{j2\delta} \quad (34)$$

where

$$\gamma' - \gamma = j2\delta \quad (35)$$

$$\delta = \sqrt{|C_{12}C_{21}| + \left(\frac{C_{11} - C_{22}}{2}\right)^2} \quad (36)$$

$$A_{1+}(x) = \frac{A_{1+}(0)}{j2\delta} \left[(\gamma' + jC_{11})e^{\gamma x} - (\gamma + jC_{11})e^{\gamma' x} \right] \quad (37)$$

$$A_{2+}(x) = \frac{A_{1+}(0)(\gamma + jC_{11})(\gamma' + jC_{11})}{j2\delta C_{12}} (e^{\gamma x} - e^{\gamma' x}) \quad (38)$$

Assume that γ 's are pure imaginary quantities (lossless). Then

$$\gamma = -j(\beta + \delta), \quad \gamma' = -j(\beta - \delta) \quad (39)$$

where

$$\beta = \left(\frac{C_{11} + C_{22}}{2}\right) \quad (40)$$

$$\delta = \sqrt{|C_{12}C_{21}| + \left(\frac{C_{11} - C_{22}}{2}\right)^2} \quad (41)$$

P_{1+} = power in $A_{1+}(x)$ mode = $2 |A_{1+}(x)|^2 = 2A_{1+}(x)A_{1+}^*(x)$.

$$P_{1+} = 2 |A_{1+}(x)|^2 = 2 |A_{1+}(0)|^2 \left[1 - \frac{1}{1 + \left(\frac{C_{11} - C_{22}}{2}\right)^2} \frac{1}{C_{12}C_{21}} \sin^2 \delta x \right] \quad (42)$$

Define F_{12} as the power transfer between modes A_{1+} and A_{2+} .

$$F_{12} = \frac{1}{1 + \left(\frac{C_{11} - C_{22}}{2}\right)^2} \frac{1}{C_{12}C_{21}} \quad (43)$$

Then the powers in A_{1+} and A_{2+} are

$$P_{1+} = 2|A_{1+}(x)|^2 = 2|A_{1+}(0)|^2 [1 - F_{12} \sin^2 \delta x] \quad (44)$$

$$P_{2+} = 2|A_{2+}(x)|^2 = 2|A_{1+}(0)|^2 - |A_{1+}(x)|^2 = |A_{1+}(0)|^2 F_{12} \sin^2 \delta x \quad (45)$$

Figure 18 shows the variation of power on the two lines for the forward mode. Note that power is first transferred from Line 1 to Line 2 beginning at $\delta x = 0$. Then from $\delta x = \pi/2$ to $-x = \pi$ power is coupled back to Line 1.

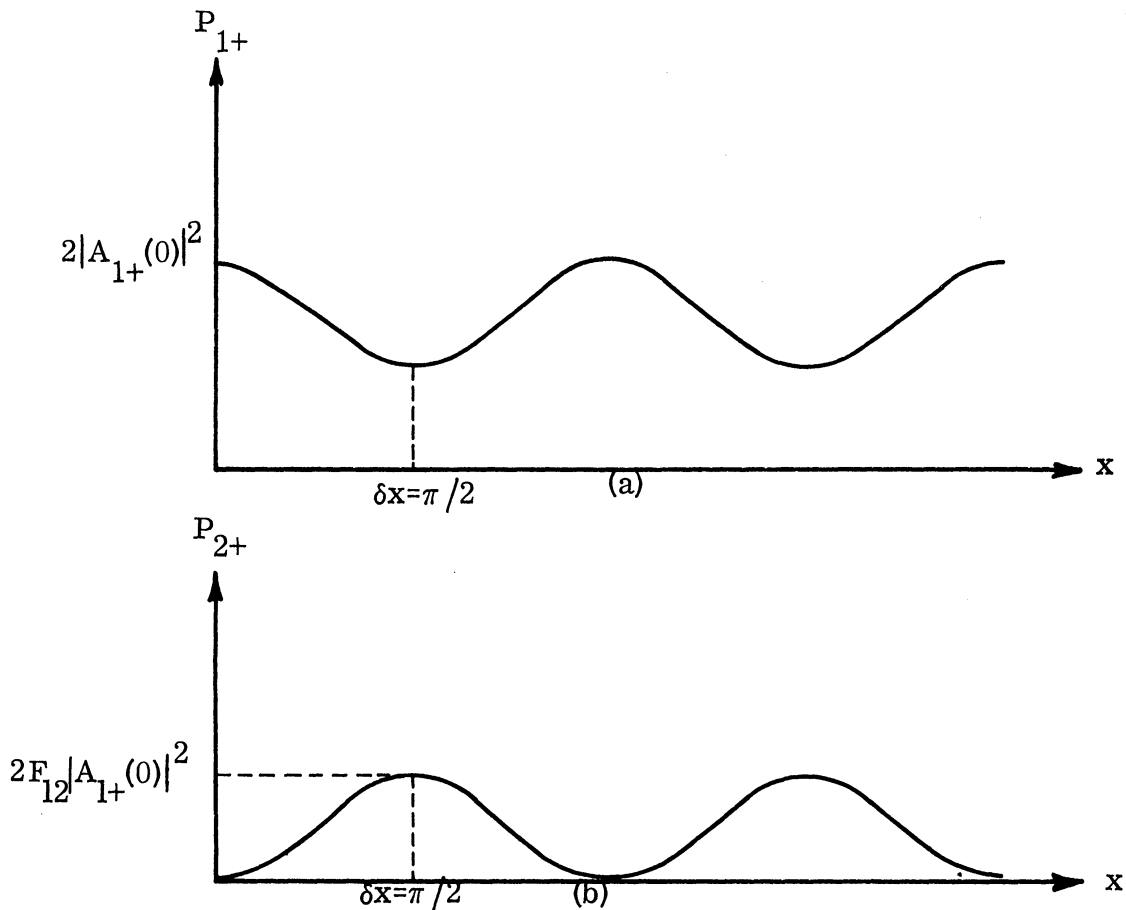


FIG. 18: ENERGY TRANSFER BETWEEN TWO COUPLED LINES.

Comparing equations (15), (16), (23) and (24) yields

$$C_{11} = j\sqrt{z_1 y_1} \quad (46)$$

$$C_{12} = \frac{z_{12}}{2\sqrt{z_1 z_2}} + \frac{y_{12}\sqrt{z_1 z_2}}{2} \quad (47)$$

$$C_{22} = j\sqrt{z_2 y_2} \quad (48)$$

$$F_{12} = \frac{1}{1 - \left(\frac{\sqrt{z_1 y_1} - \sqrt{z_2 y_2}}{2} \right)^2} \frac{1}{\left(\frac{z_{12}}{2\sqrt{z_1 z_2}} + \frac{y_{12}\sqrt{z_1 z_2}}{2} \right)^2} \quad (49)$$

if

$$\begin{array}{lll} z_1 = -j\omega L_1 & z_2 = -j\omega L_2 & Z_1 = \sqrt{L_1/C_1} \\ y_1 = -j\omega C_1 & y_2 = -j\omega C_2 & \\ z_{12} = -j\omega M & y_{12} = -j\omega N & Z_2 = \sqrt{L_2/C_2} \end{array}$$

where L_1 , C_2 , M and N are line parameters per unit length of 1 meter.

Then

$$F_{12} = \frac{1}{1 + \left(\frac{\omega\sqrt{L_1 C_1} - \omega\sqrt{L_2 C_2}}{2} \right)^2} \frac{1}{\left(\frac{j\omega M}{2\sqrt{\frac{L_1 L_2}{C_1 C_2}}} + \frac{j\omega N \sqrt{L_1 L_2 / C_1 C_2}}{2} \right)^2} \quad (50)$$

Optimum coupling occurs if $\omega\sqrt{L_1 C_1} = \omega\sqrt{L_2 C_2}$ and F_{12} equals one. This means total power transfer occurs.

$$P_{1+} = 2|A_{1+}(x)|^2 = 2|A_{1+}(0)|^2 \left[1 - \sin^2 \left(\frac{\omega M}{2\sqrt{L_1 L_2 / C_1 C_2}} + \frac{\omega N \sqrt{L_1 L_2 / C_1 C_2}}{2} \right) x \right] \quad (51)$$

$$P_{2+} = 2|A_{2+}(x)|^2 = 2|A_{1+}(0)|^2 \sin^2 \left(\frac{\omega M}{2\sqrt{L_1 L_2 / C_1 C_2}} + \frac{\omega N \sqrt{L_1 L_2 / C_1 C_2}}{2} \right) x \quad (52)$$

The coupling of the other mode combinations mentioned on page 29 is not given here but will be included as an appendix to the final report. There is very low coupling for Cases (2) and (3) involving, in each case, opposite modes. The coupling for Case (4) involving backward modes only on the 2 lines, is formulated in the same general manner as Case (1)

4.2 Experiments on Energy Transfer and Radiation

The experimental program will be used to confirm the energy transfer conditions prevailing for a ferrite radiator which is fed in a manner corresponding to one transmission line being coupled to another. To date, the experimental data acquired have not been sufficient to confirm the mathematical relations.

Certain definitive experiments were run using a spiral transmission line for Line No. 1, and various pitches and diameters of such a transmission were used. Also, measurements were used at various spacings of the transmission to the ferrite slab. Radiation from spiral transmission line was not wanted and therefore shielding was introduced so as to make measurements upon the radiation field of the ferrite slab alone. This meant that an objective was to study the ferrite slab as an end fire radiator, knowing that all energy so radiated had to be coupled at the second transmission line from Line No. 1. It is expected that the optimum coupling situation will take place when the phase velocity along the axis of Line No. 1 is very near, or slightly in excess of the phase velocity for a wave traveling in the ferrite

slab. This criterion is one similar to that commonly used in traveling wave tubes. The results of this experimentation are not entirely conclusive at the present time. It is expected that in the final report it will be possible to summarize worthwhile results of this experimental program.

It is possible that a test set-up such as used in this study may be used to devise a method of accurately ascertaining the produce of μ and ϵ , since the optimal point for energy transfer may possibly be used as an indicator for the matching of phase velocities.

V

SLOT ANTENNAS WITH RIDGES OR IRISES

In continuing the research on ferrite loaded slot antennas that was initiated by this laboratory on earlier contracts, it was decided to modify the slot antenna, if possible, to allow a wider bandwidth or lower frequency of operation for the same given outside dimensions of the slot antenna. Well-known properties of the ridged waveguide, as well as preliminary experiments performed last year, indicated a possible potential for broadbanding or lowering the frequency of operation of the slot antenna. The following study was entirely experimental and consisted of inserting various ridges and metal irises into the ferrite-filled slot antenna and noting the changes and impedance as shown in the Smith Chart of the impedance to the antenna. To reduce the complexity of the data presentation, all Smith Chart grids have been suppressed except for a VSWR scale.

5.1 Assumptions of the Study

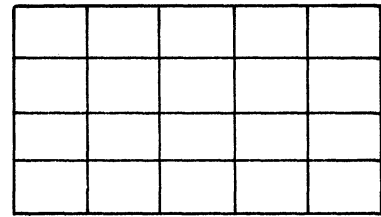
Several assumptions were made in processing the impedance data for a 'bandwidth'.

- 1) Tuners were usually not used experimentally.
- 2) A VSWR circle = 3 was placed about each desired grouping of impedance points to obtain bandwidth (equivalent to the use of a wideband phase shifter and a wideband impedance transformer).
- 3) No further distortion of the impedance plots by compensation tuning was allowed.

Actually, with compensation tuning, somewhat larger bandwidths might well be obtained.

5.2 Solid Ferrite Loaded Antenna

Figure 19a shows an impedance Smith Chart diagram of the input impedance to the slot antenna entirely filled with solid ferrite blocks. All ferrite is solid



all ferrite blocks

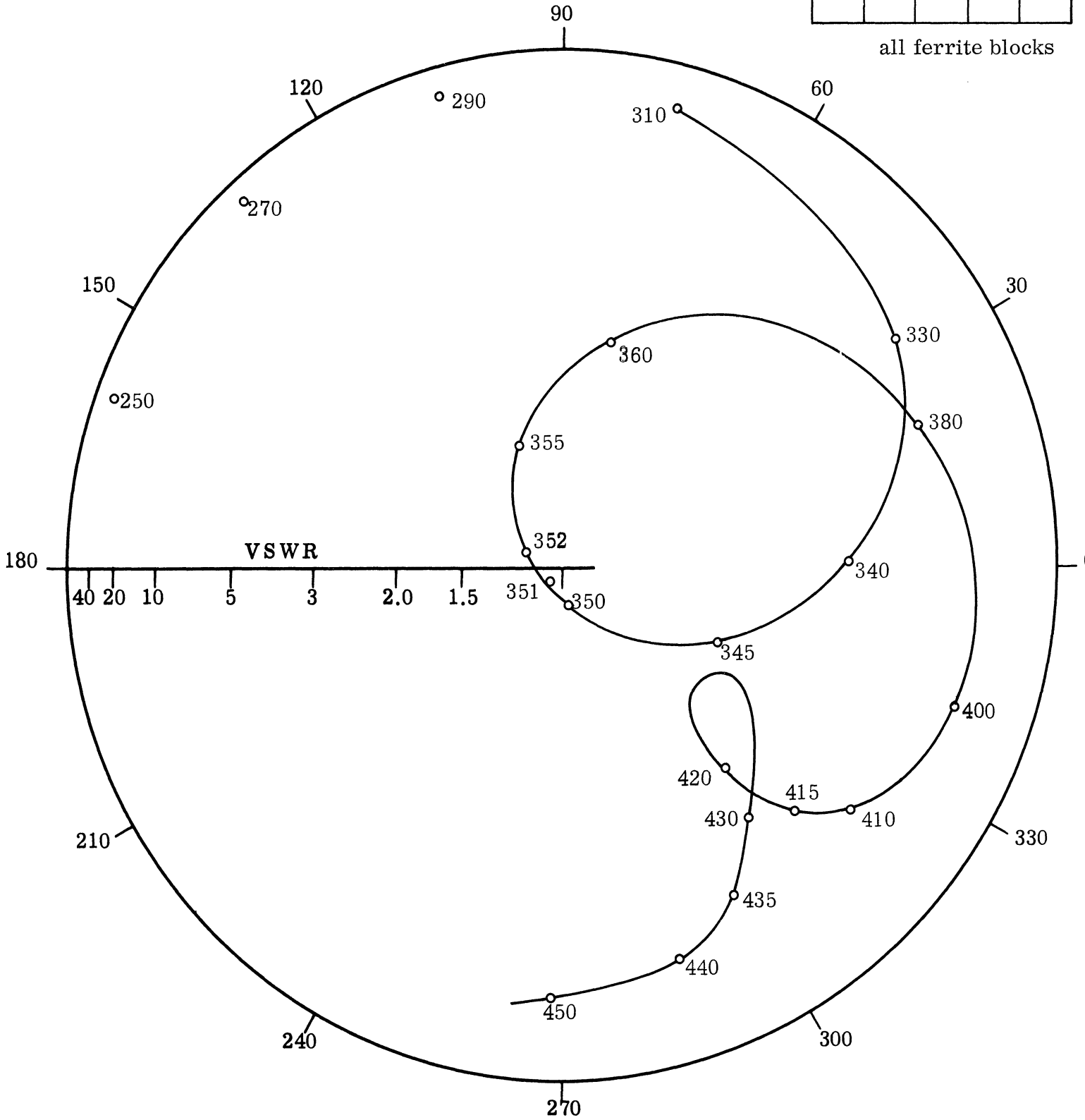


FIG. 19a: IMPEDANCE DIAGRAM OF SLOT ANTENNA LOADED ENTIRELY WITH SOLID FERRITE (Frequency MHz)

EAF-2 material, the properties of which are summarized in Section IV of this report. This slot antenna, entirely filled with solid ferrite, has been thoroughly analyzed by Adams (1964). The operating frequency of this antenna is 352 MHz and the bandwidth is 18 - 20 MHz for a VSWR below 3, as may be seen by drawing a circle (VSWR=3) about the origin of the Smith Chart. Nevertheless, this antenna, if its impedance would be transformed properly, could operate from approximately 333 MHz to 383 MHz (50 MHz bandwidth), as may be seen by shifting the loop located in the upper right-hand portion of the Smith Chart clock-wise to the real impedance axis (e. g. by a wideband phase shifter) and then drawing a VSWR=3 circle about this loop, keeping in mind that the diameter of this circle changes with position on the Smith Chart. The 50 MHz bandwidth is therefore roughly the optimum bandwidth that could be achieved by this antenna with a wideband impedance transformation, but without other optimizing circuits. In order to show the effect of a simple, but very narrow-band transformer in the form of a double stub tuner, this solid ferrite loaded slot antenna was tuned with a double stub tuner in an attempt to move the upper right-hand loop to the central region. Figure 19b shows the resulting input impedance, and indicates a drastic change has taken place in the shape of the curve due to the additional phase shift of the double stub tuner. The phase reference for the original solid ferrite loaded slot antenna was at the input to the 'N' connector mounted directly on the antenna. The phase reference for the antenna shown in Fig. 19b with the double stub tuner attached, was at the input to the double stub tuner, a considerable distance from the actual antenna. This caused an additional phase shift down by a more rapid rotation of the input impedance with change in frequency. This second curve (Fig. 19b) has much less optimized bandwidth (approximately 23 MHz) for only slightly lower center frequency. One can conclude that transformation of the input impedance with this particular setting of the double stub tuner, and probably with most other settings, would not be satisfactory for transforming the input impedance in the manner desired for increasing bandwidth or lowering frequency of operation.

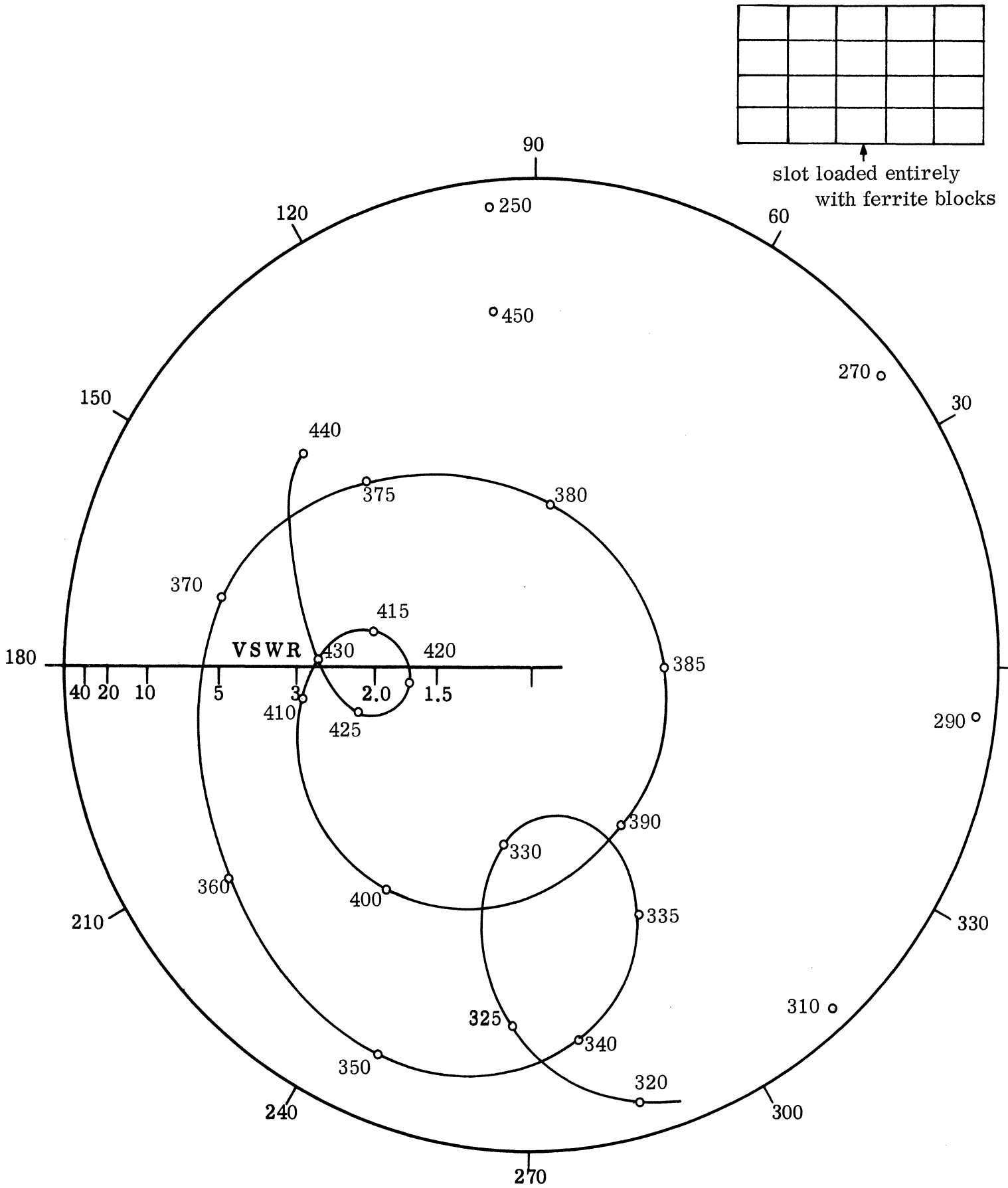


FIG. 19b: IMPEDANCE DIAGRAM OF SLOT ANTENNA LOADED ENTIRELY WITH SOLID FERRITE. DOUBLE STUB TUNER USED. (Frequency MHz)

5.3 Loaded Slot Antenna with Irises

Earlier studies by this laboratory indicated that partial blocking of the loaded antenna aperture significantly changed the input impedance of the antenna such that the bandwidth (as measured by magnitude of VSWR) was improved. Figure 20a shows the effect of two irises which are actually aluminum tape covering the front ends of several of the ferrite blocks used in loading the slot antenna. The actual input impedance (referenced to 50 ohms) is poor by any standard. Nevertheless, the loop on the left is interesting since it occurs at such low frequencies. A circle for VSWR corresponding to three indicates a possible transformed bandwidth of 16 MHz centered at approximately 259 MHz. Another attempt at transforming the impedance chart with a double stub tuner had the effects shown in Fig. 20b where the lower frequency of operation loop has clearly been moved closer to the center of the Smith Chart. Although the loop is larger in radius, the bandwidth of 20 MHz around 261 MHz is approximately preserved. The reason that the lower frequency of operation loop has not been placed at the center of the Chart is an experimental difficulty in controlling the placement of this loop with the double stub tuner (which is after all, essentially a narrow band device) In summary, the possibility of operating at a frequency approximately 100 MHz lower than the original frequency of the ferrite-filled antenna by simply using an iris, is interesting and potentially useful, but it is accomplished at the expense of bandwidth.

Another iris experiment (Fig. 20c) involved covering the lower row of ferrite blocks. This produced practically no impedance changes in the lower frequency of operation ; a bandwidth of 42 MHz around 356 MHz is shown and this iris was therefore discarded.

In the final iris experiment (Fig. 20d) the iris covered the lower three blocks of the center column. The low frequency loop in the upper left diagram has a potential VSWR = 3 bandwidth of 13 MHz centered around 273 MHz, which is again potentially useful in decreasing the operating frequency, although it drastically reduces the bandwidth.

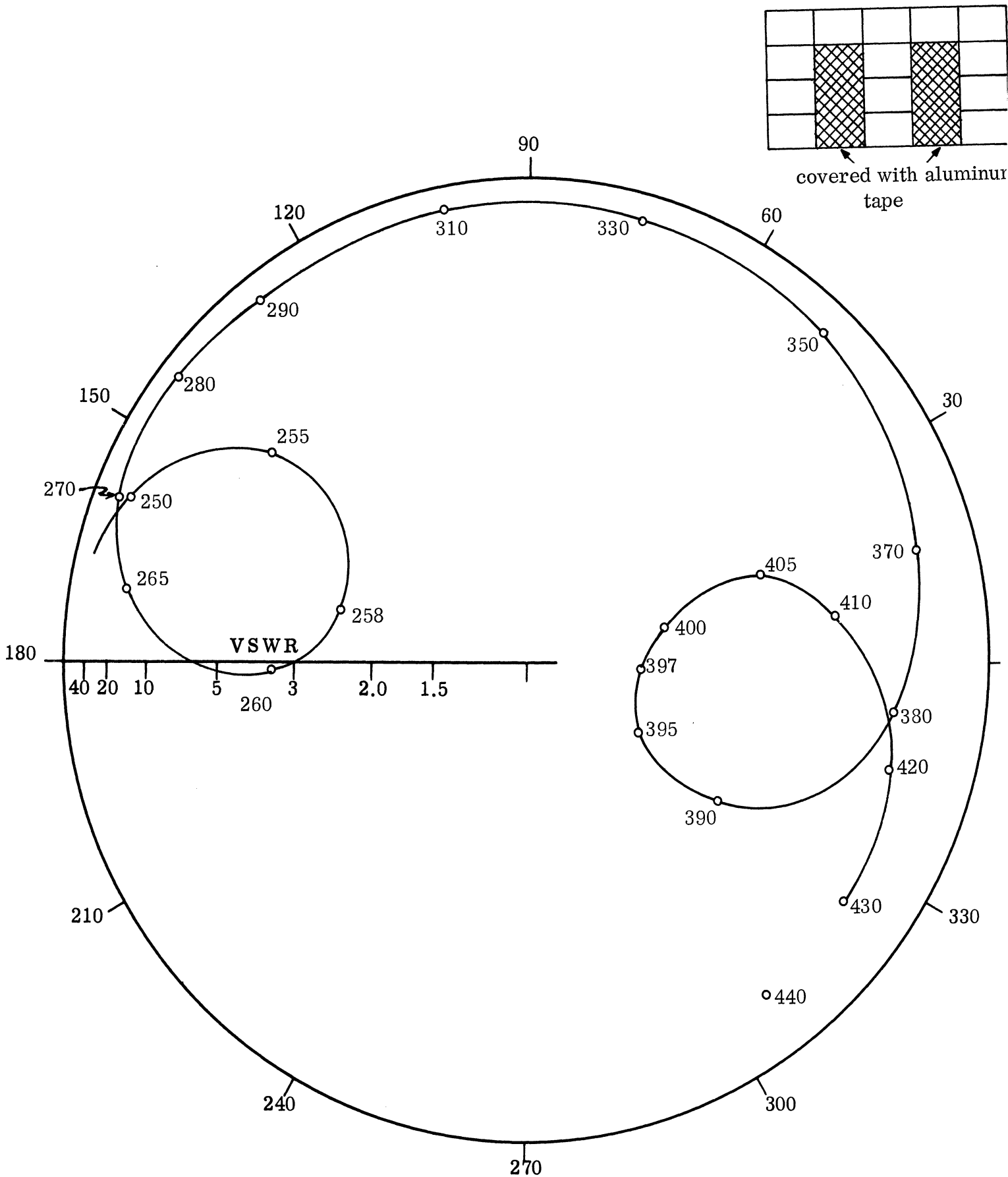


FIG. 20a: IMPEDANCE DIAGRAM OF SOLID FERRITE LOADED SLOT ANTENNA WITH IRIS (Frequency MHz).

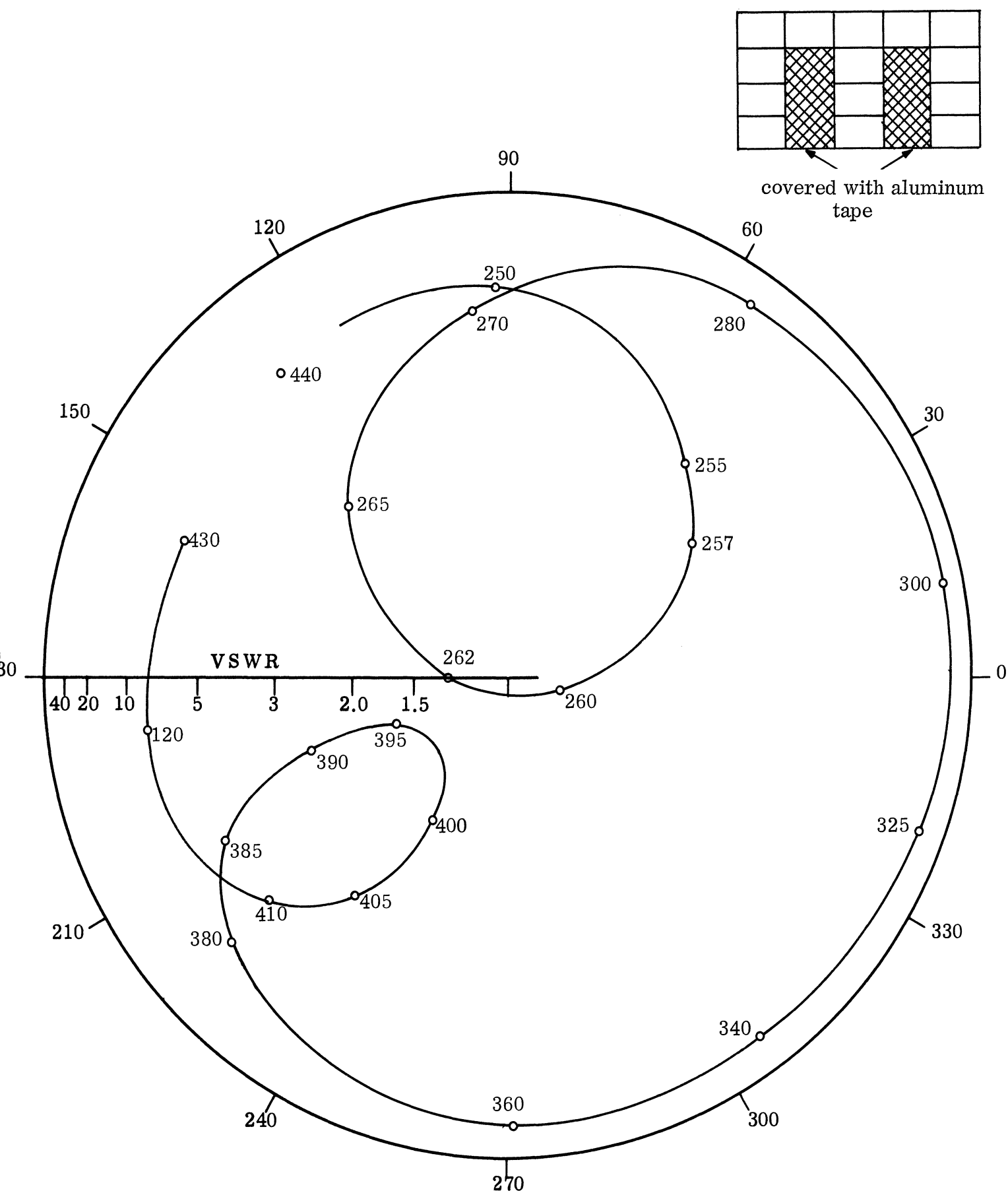


FIG. 20b: IMPEDANCE DIAGRAM OF SOLID FERRITE LOADED SLOT ANTENNA WITH IRIS. DOUBLE STUB TUNER USED. (Frequency MHz)

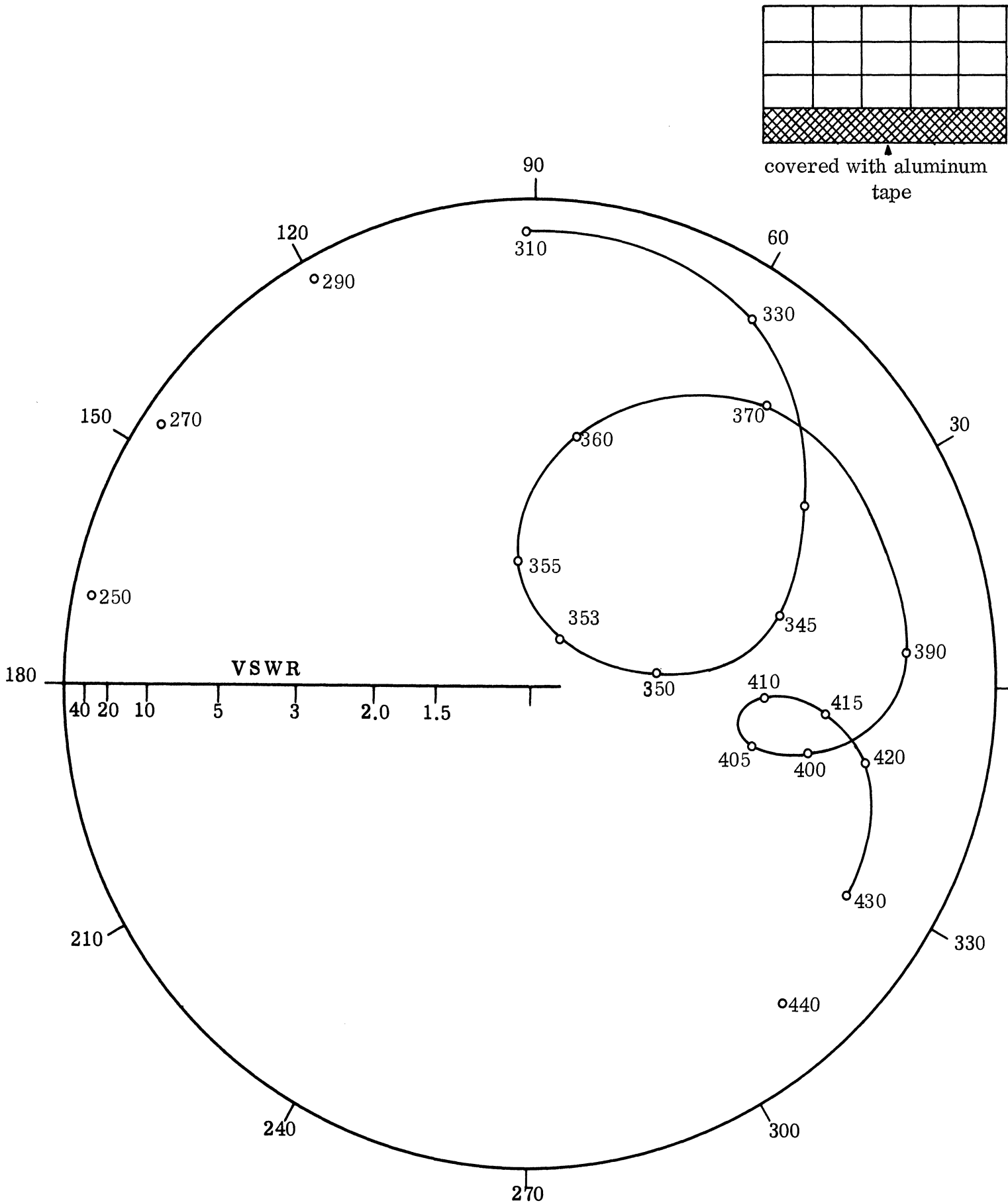


FIG. 20c: IMPEDANCE DIAGRAM OF SOLID FERRITE LOADED SLOT ANTENNA WITH IRIS (Frequency MHz).

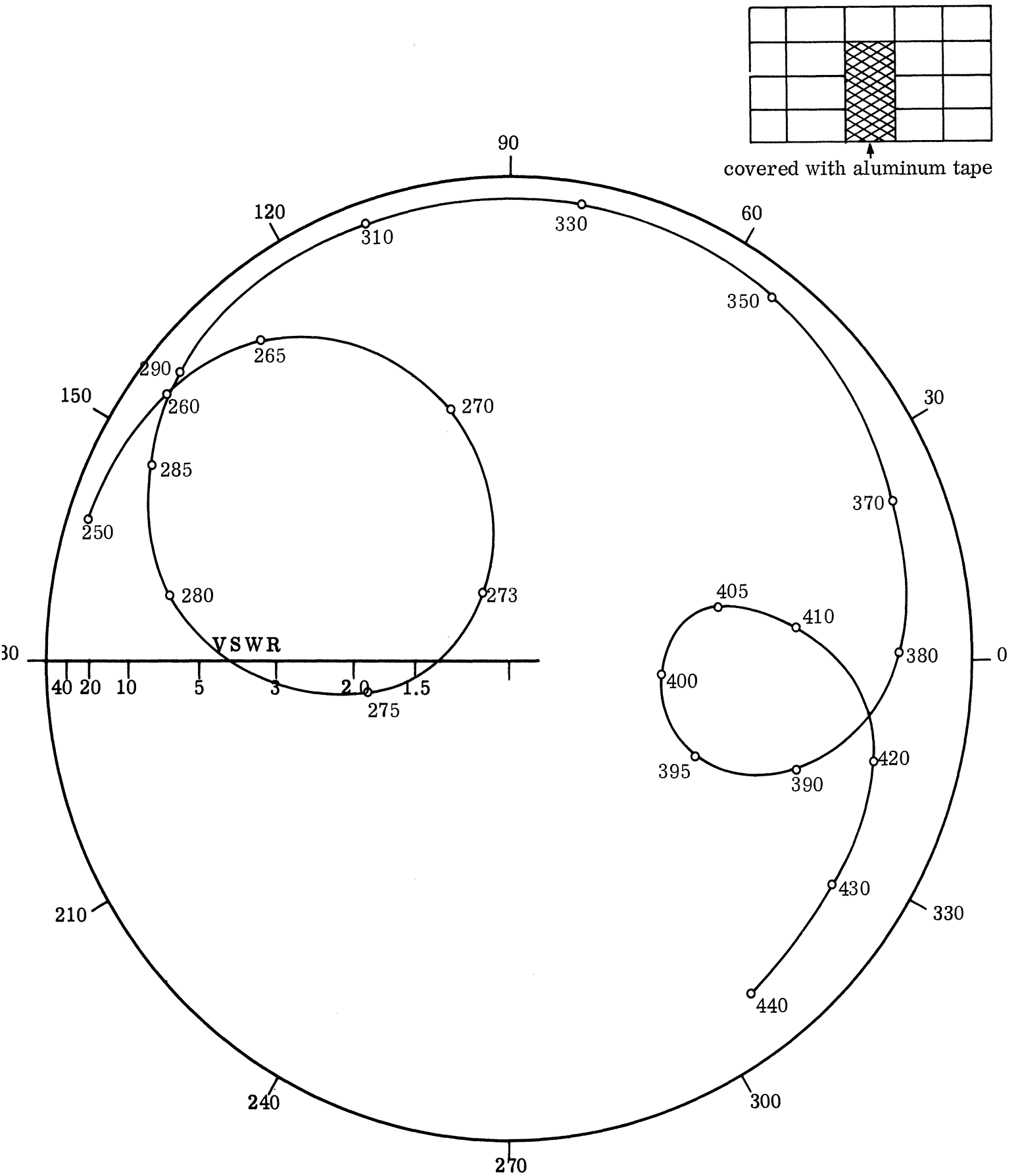


FIG. 20d: IMPEDANCE DIAGRAM OF SOLID FERRITE LOADED SLOT ANTENNA WITH IRIS (Frequency MHz).

Experiments attempted using side irises, were unsuccessful.

In conclusion, irises appear to act as very narrow band tuners since reflections from the iris (sensitive to frequency) are being used; nevertheless, lower frequencies of operation are achievable with apparently greater bandwidths than would be obtained by using an external tuner.

5.4 Ridged Loaded Slot Antennas

Because of the increased bandwidth and lower operating frequency of the ridged waveguide, a series of slot loaded antenna experiments was initiated with various ridges created by steel or aluminum blocks replacing the ferrite blocks usually used in loading the slot antennas. It is important to note that the ridges were used without regard for possible improvement in matching the input probe impedance, even though the input probe was specifically designed only for the fully filled ferrite slot antenna. Figure 21a (inset) shows two metal ridges extending down to the lower side of the antenna where upper and lower are distinguished in this antenna by the fact that an electric monopole probe feed is used to excite the slot antenna and is inserted in the center of the antenna from the top. Figure 21a also shows the effect of the ridges on the input impedance and indicates again a substantial lowering in the lowest operating frequency obtainable from the slot waveguide. A bandwidth of 35 MHz around 291 MHz is achieved. This is felt to be a significant improvement in antenna performance.

The second set of ridges used (Fig. 21b) consists of two sets of two steel blocks or ridges substituted for the center ferrite blocks. Figure 21b shows then the effect on the input impedance of these center ridges and indicates an operating bandwidth of 50 MHz around 330 MHz. The resulting 50 MHz is essentially unchanged from the completely loaded ferrite slot antenna and the center frequency of 330 MHz is not much different from the original 350 MHz. This loading, therefore, it not considered to be particularly useful.

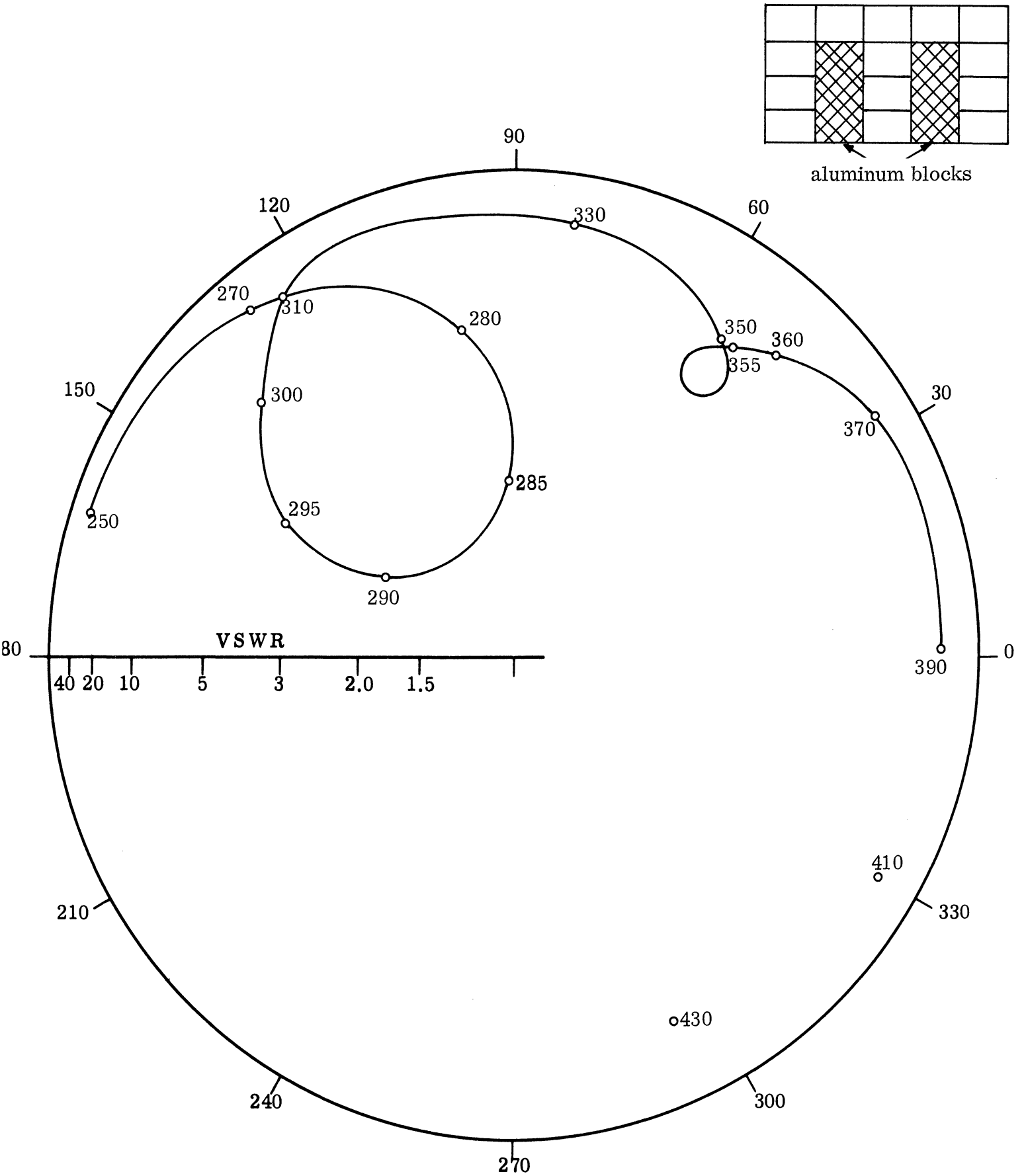


FIG. 21a: IMPEDANCE DIAGRAM OF SOLID FERRITE LOADED SLOT ANTENNA WITH RIDGES (Frequency MHz).

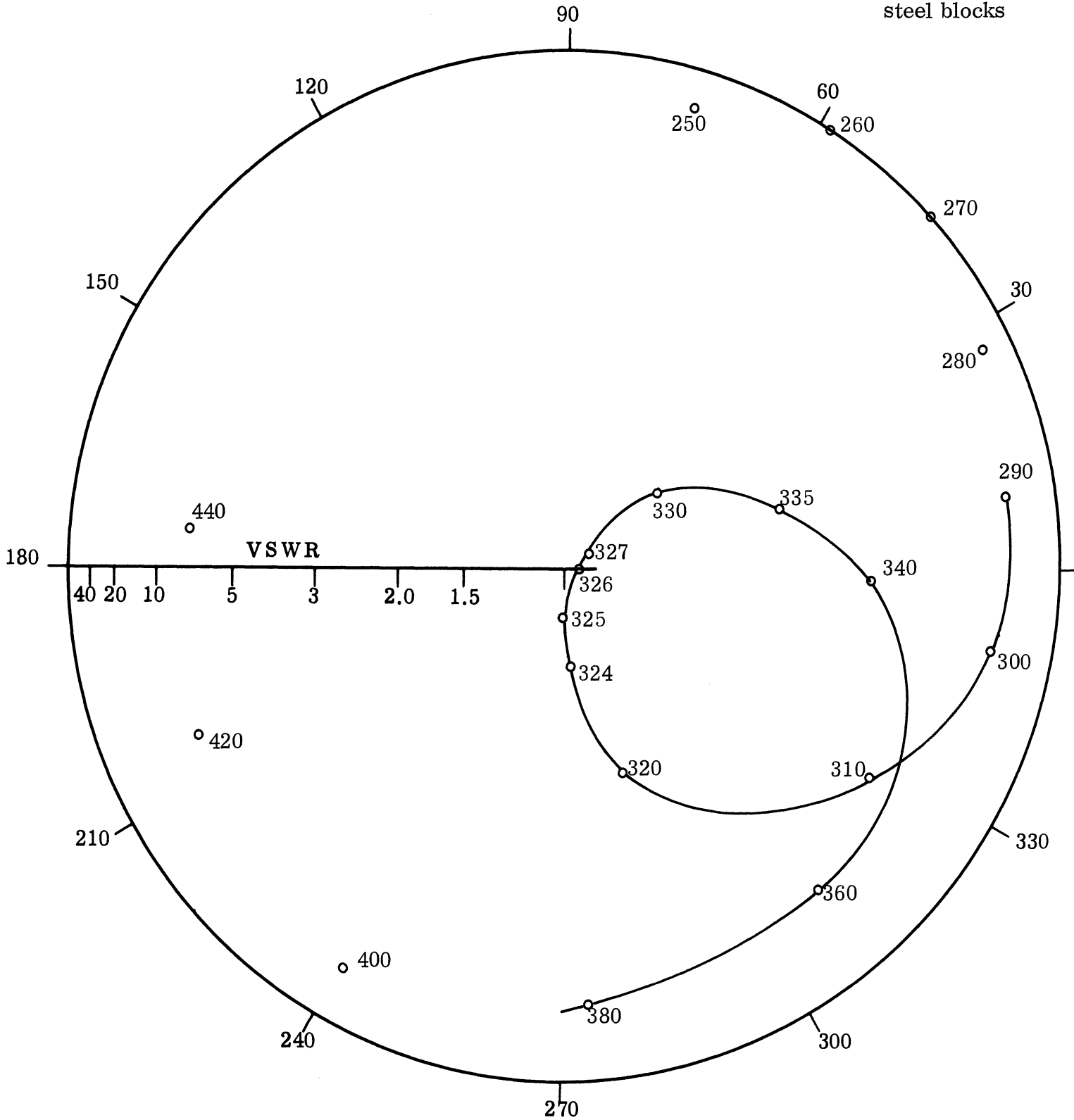
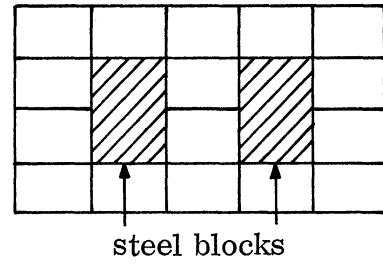


FIG. 21b: IMPEDANCE DIAGRAM OF SOLID FERRITE LOADED SLOT ANTENNA WITH RIDGES (Frequency MHz).

Another double ridge slot antenna (Fig. 21c) shows significant improvement in the lower operating frequency with a possible transformed bandwidth of 44 MHz around 317 MHz. This is a shift downward of 41 MHz in operating bandwidth, a small but possibly useful shift.

Figure 21d shows an asymmetrical ridged arrangement used in the loaded slot antenna and the resulting impedance diagram. Again, an important lowering in the operating center of frequency is noted. The resulting bandwidth of 27 MHz around 292 MHz may be useful. The higher frequency loop on the Smith Chart (around 360 MHz) is not considered valuable.

Many somewhat less successful experiments were attempted using ridged slot waveguide. Figures 21e, 21f and 21g show such loadings. Although the curves all appear single-looped and reasonably simple, they do not appear to have value either in lowering the center of operating frequency or increasing the bandwidth even when impedance transformations to the center of the Smith Chart are considered. Ridges extending down from the top and ridges covering all (or almost all) of the height of the slot were unsuccessful. Finally, various schemes of replacing ferrite blocks with balsa wood were attempted, the balsa acting essentially as free space or air. Such schemes invariably ended in raising, rather than lowering, the center of the operating frequency.

5.5 Conclusions and Summary

Table III summarizes the results of the ridged slot antenna studies. Figures 20a, 20b, 21a, 21c and 21d showed configurations which were useful in lowering the operating frequency while maintaining a reasonable bandwidth. In all of these, it is noted that a single or double arm iris or ridge in the waveguide is used, extending to the bottom of the waveguide and partially to the top. Most irises or ridges are three blocks high (out of the four) and arranged in a central column. A decrease in center frequency of 60 MHz is not difficult to attain. Ridges appear to have potentially a wider bandwidth than irises.

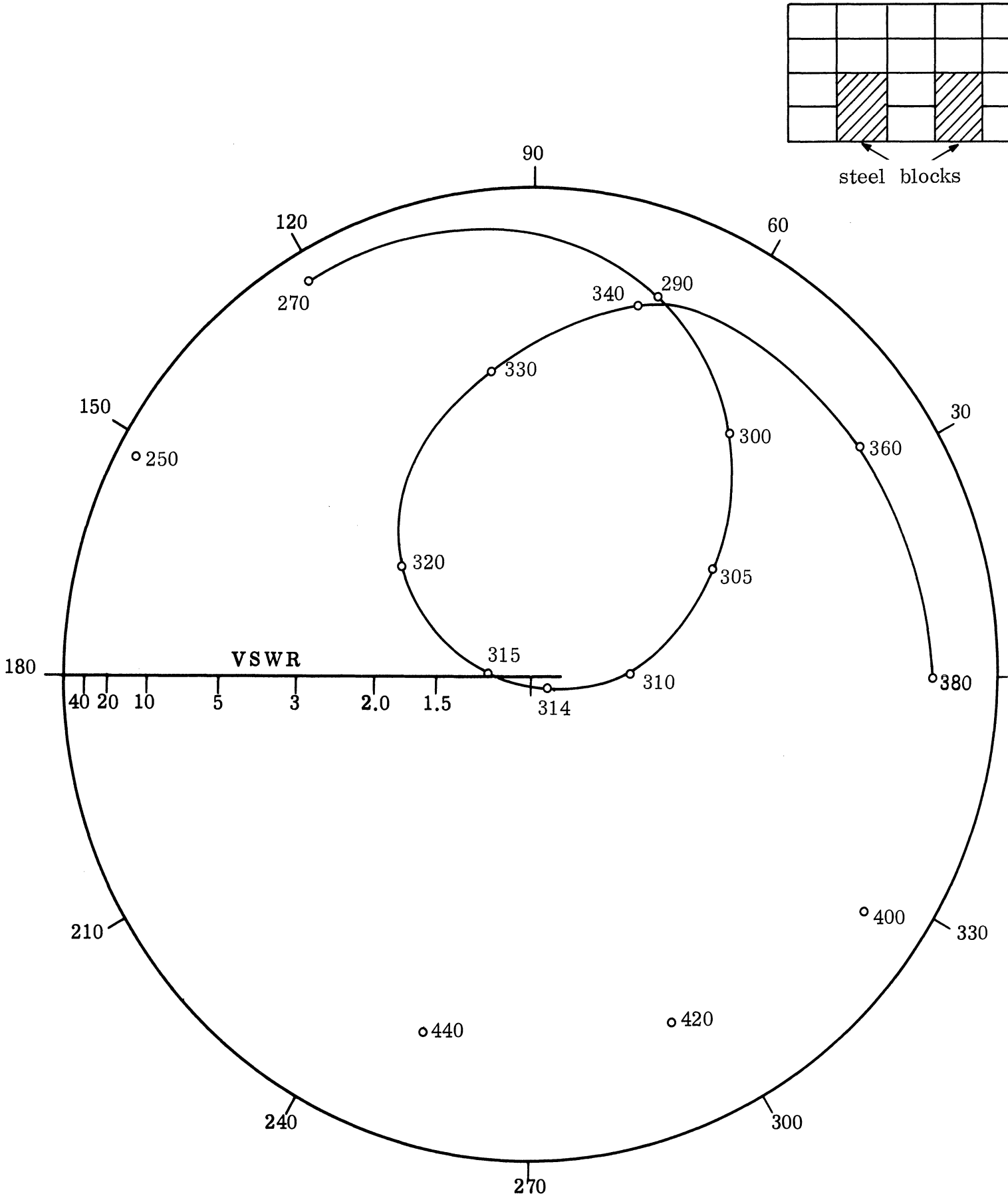


FIG. 21c: IMPEDANCE DIAGRAM OF SOLID FERRITE LOADED SLOT ANTENNA WITH RIDGES (Frequency MHz).

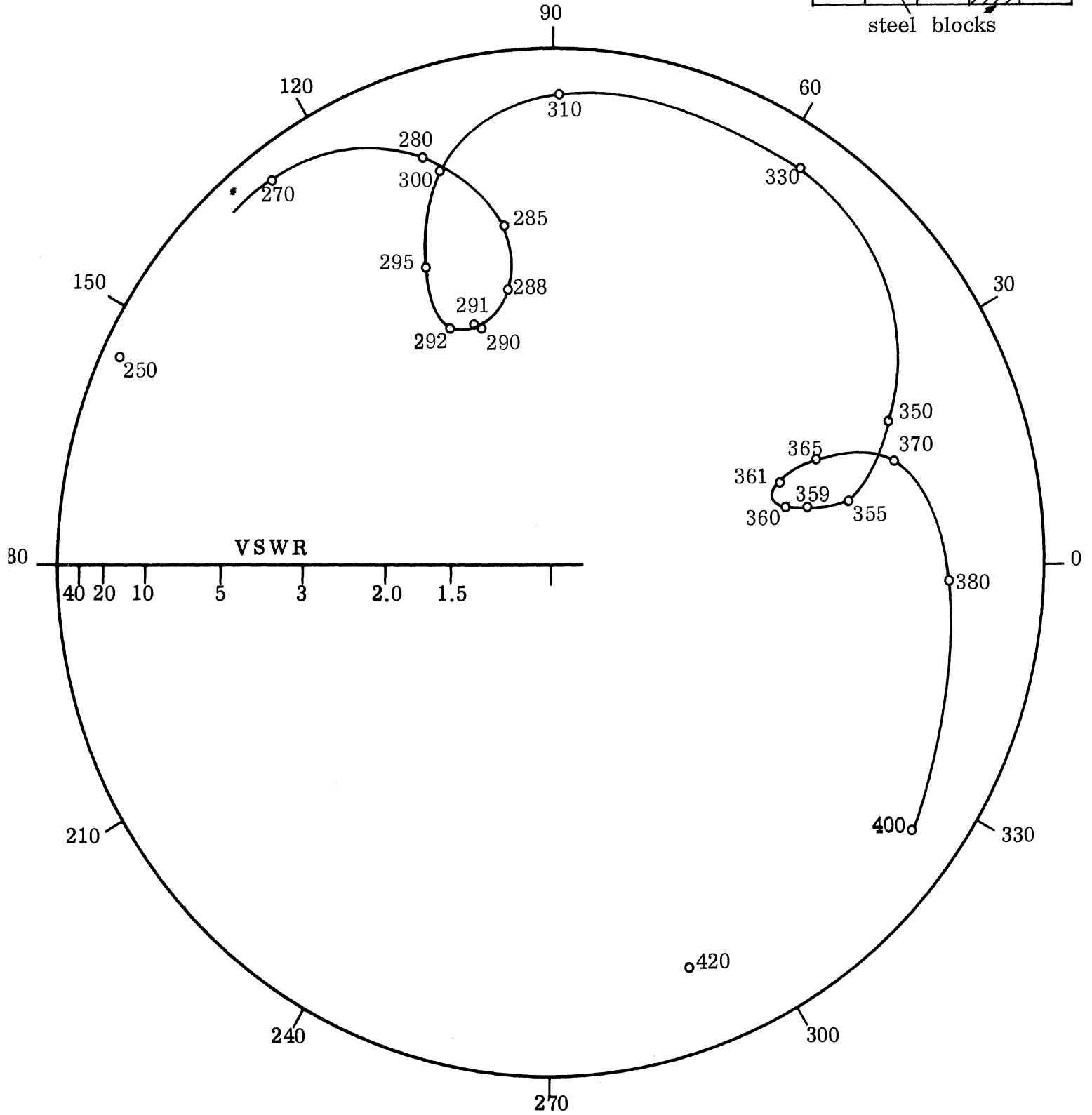
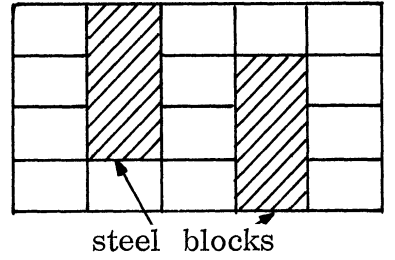


FIG. 21d: IMPEDANCE DIAGRAM OF SOLID-FERRITE LOADED SLOT ANTENNA WITH RIDGES (Frequency MHz).

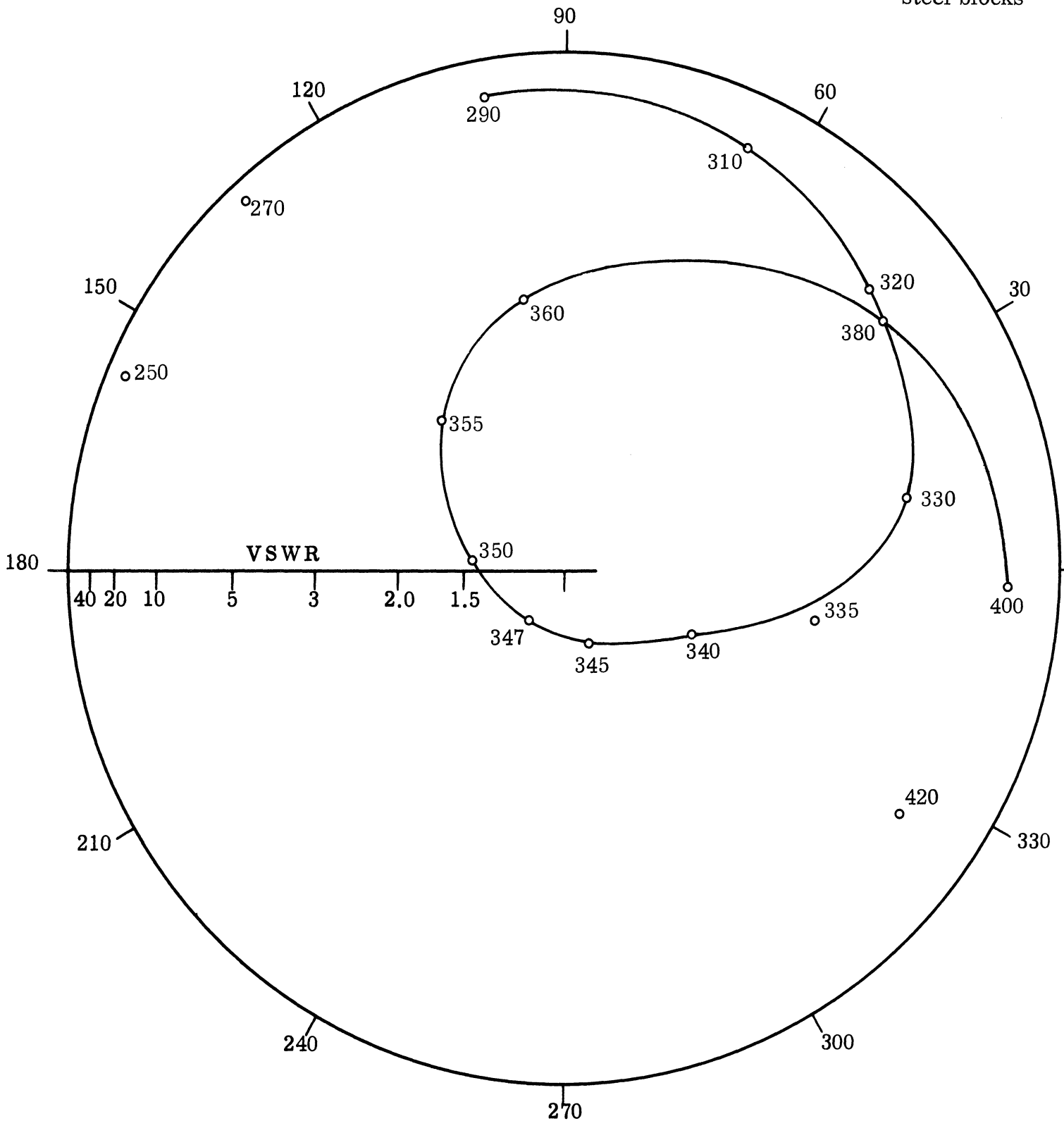
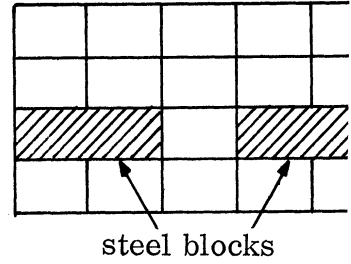


FIG. 21e: IMPEDANCE DIAGRAM OF SOLID FERRITE LOADED SLOT ANTENNA WITH RIDGES (Frequency MHz)

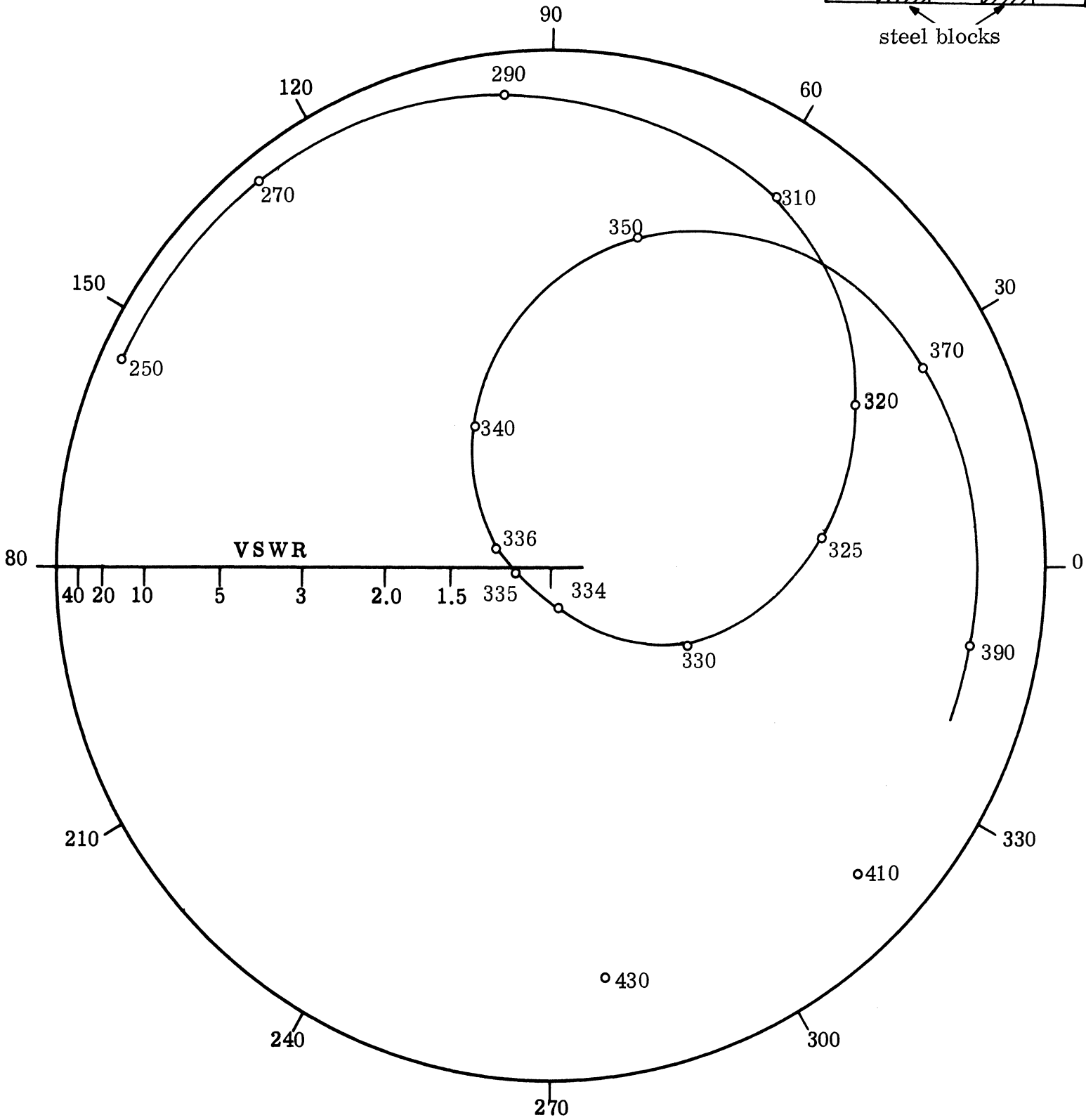
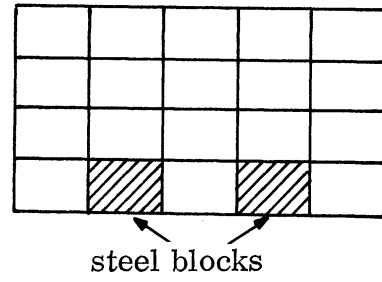


FIG. 21f: IMPEDANCE DIAGRAM OF SOLID FERRITE LOADED SLOT ANTENNA WITH RIDGES (Frequency MHz).

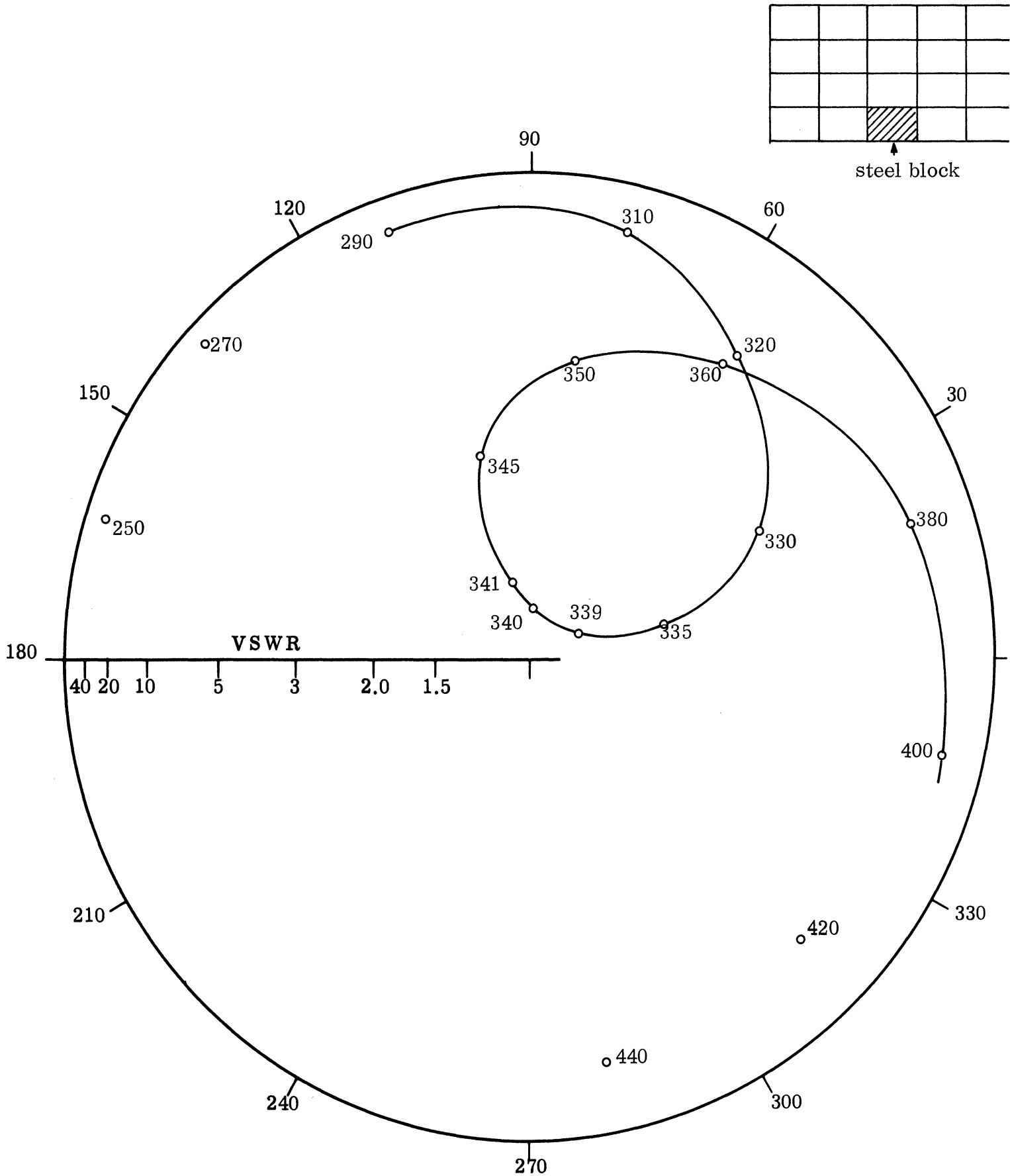


FIG. 21g: IMPEDANCE DIAGRAM OF SOLID FERRITE LOADED SLOT ANTENNA WITH RIDGES (Frequency MHz).

TABLE III: SUMMARY OF RIDGE SLOT ANTENNAS

| Figure No. | Center Frequency (MHz) | Bandwidth (MHz) | Remarks |
|------------|------------------------|-----------------|----------------|
| 19a | 352 | 18 | No tuner |
| 19a | 358 | 50 | Optimum tuning |
| 19b | 344 | 23 | Optimum tuning |
| 20a | 259 | 16 ⁺ | Optimum tuning |
| 20b | 261 | 20 ⁺ | Optimum tuning |
| 20c | 356 | 42 | Optimum tuning |
| 20d | 273 | 13 | Optimum tuning |
| 21a | 291 | 35 ⁺ | Optimum tuning |
| 21b | 330 | 50 | Optimum tuning |
| 21c | 317 | 44 ⁺ | Optimum tuning |
| 21d | 292 | 27 ⁺ | Optimum tuning |
| 21e | Not potentially useful | | Optimum tuning |
| 21f | Not potentially useful | | Optimum tuning |
| 21g | Not potentially useful | | Optimum tuning |

⁺ Indicates potentially useful results.

Although the impedance diagrams for various configurations of ridges and irises appear useful, the efficiency of the antenna as a radiator must yet be investigated. It is assumed that the antenna patterns will be the usual dipole patterns since the antennas are much smaller than 1λ . Attempts at measuring efficiency with the usual 'hat reflector' method were unsuccessful. It is planned to use direct field strength measurements to determine efficiency.

In order to achieve the necessary impedance transformation to make the ridges or irises useful in transforming antenna impedance, a better backing cavity should be designed for each ridge or iris configuration so that a real impedance is faced by the probe rather than the imaginary or partially imaginary impedances now seen. As mentioned, the probe was designed for a fully loaded cavity rather than the partially loaded cavities tested. In addition it may be necessary to specifically design the ridges or irises such that excessive energy concentrations are avoided, since energy concentrations lead to great losses in ferrite structures.

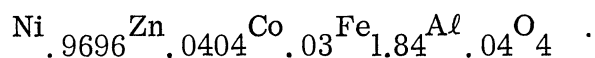
VI

FERRITE MATERIALS

During this reporting period attention has been given to extending the use of ferrite loading to lower frequencies (down to 30 MHz). With this in mind, additional ferrite material has been purchased (e. g. Q-3, from Indiana General). Some of the experiments in preliminary design are based upon forms of this material which have been readily available. This material appears to have reasonably good electrical and magnetic characteristics. Some of the designed experiments have been limited because of the availability of ferrite material in proper form. The Q-3 material has been ordered in three forms: 1) Stick (2.85"x0.5"x0.12"); 2) Cylindrical Rod (1.937"x0.25"), and 3) Circular Toroids (0.5" OD x 0.28" ID x 0.25" thick).

The restriction on the form of the material has resulted in certain experiments being scheduled before others. Ultimately, it is expected that powdered type Q-3 ferrite will be available. This will be obtained by using some of the solid forms mentioned above and pulverizing them through the use of a ball mill. Ferrite type Q-3 appears to have excellent characteristics below a frequency of 200 MHz. Available information on this ferrite, as obtained from advertising circulars, is somewhat controversial. The characteristics are shown in Fig. 22 and will be discussed later. It is anticipated that measurements by this laboratory on the characteristics of the material will supplant the reported values with verified data.

In addition to Q-3, a considerable study has been made of other available ferrites. Table IV gives names and manufacturer for several selected high-Q ferrites. The first ferrite, EAF-2, is the one presently used in our ferrite-loaded antenna studies. Its properties have been thoroughly measured by this laboratory. All of the work involving experimental tests of antennas loaded with powdered ferrite have used this material either in powdered or solif form. Its formula is



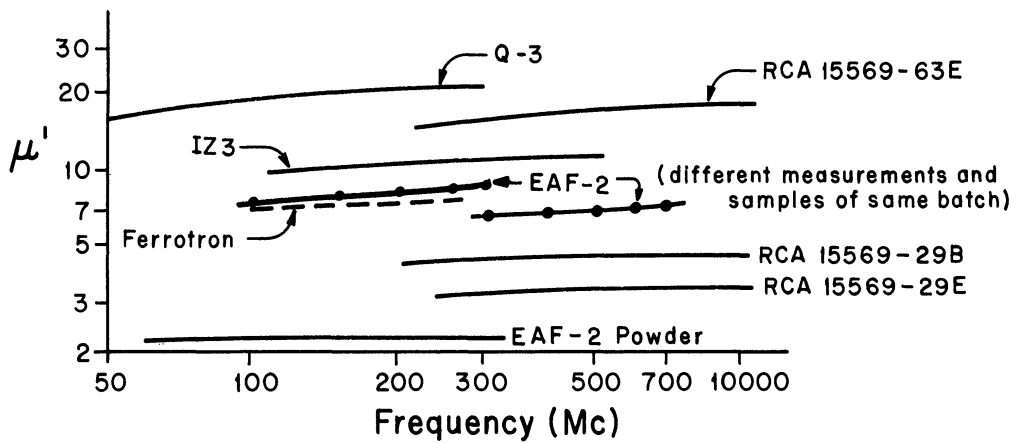
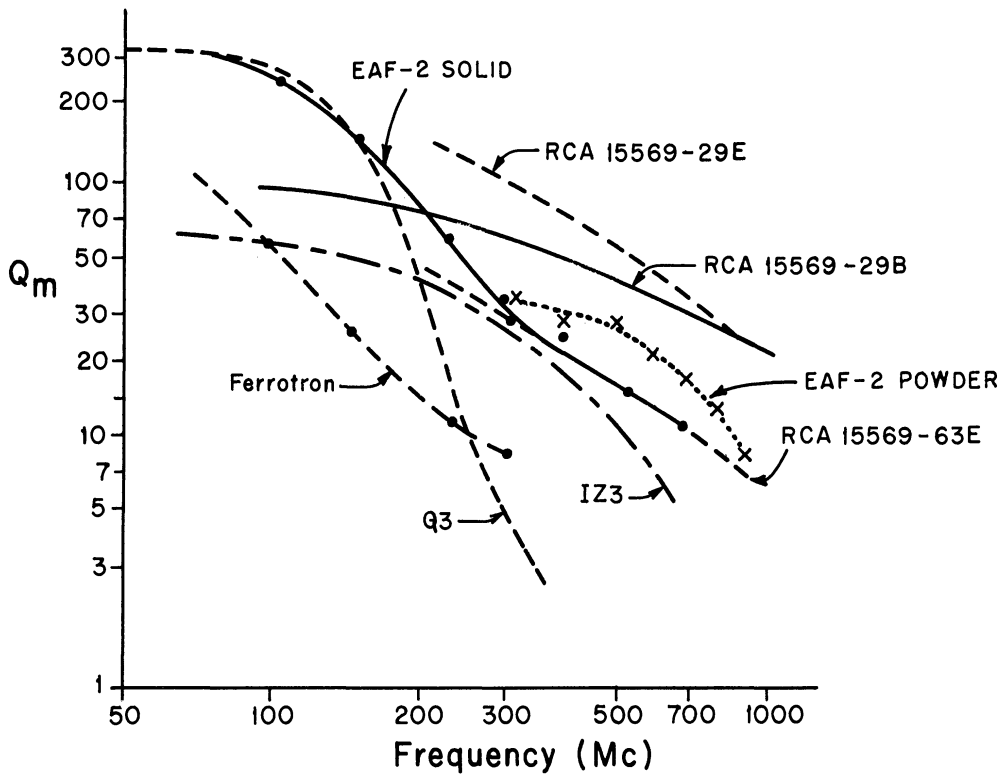


FIG. 22: Q AND μ' FOR VARIOUS FERRITES. DOTS AND X's INDICATE U OF MICHIGAN MEASUREMENTS.

TABLE IV: SELECTED HIGH-Q FERRITES

| Ferrite | Manufacturer | Remarks |
|------------------|-----------------|---|
| EAF-2 | Motorola | Production not repeatable. No longer available. Tested at U of M. |
| Q-3 | Indiana General | Several sizes on order. To be tested. |
| Ferrotron | Polymer Corp. | Not a ferrite. Iron impregnated plastic. Excellent at high temperatures. Q_m and μ' measured at U of M. |
| IZ3 | Ferroxcube | Measured resonance in ϵ' at 100 MHz. |
| RCA 15569 Series | RCA | Tested for USAEC by RCA. RCA does not produce. Formula said to be reproducible. |

The EAF-2 material (designated in previous reports as type A) has been satisfactory for experiments on earlier contracts. It is the same material which was used in the detailed studies of the rectangular cavity-backed slot. The temperature dependence of this material has been reported in Lyon et al (1964). Attempts to purchase more of this material have failed. This may be due to the difficulty experienced in reproducing the high quality of the first batch.

The second ferrite, Q-3, has already been discussed.

The third ferrite, Ferrotron, has been recently tested by this laboratory. The tests did not substantiate its advertised high-Q properties at 300 MHz and above.

The fourth and fifth ferrites have not been tested by this laboratory except for brief dielectric tests on IZ3. The RCA materials (1963) are experimental and were developed for the U S Army Signal Corps. Currently, RCA is not manufacturing this ferrite, although sufficient information is available for others to manufacture it. Figure 22 shows the Q_m (magnetic Q) and μ' properties for the various ferrites

investigated. It can be seen from the Q_m curves that the present EAF-2 ferrite from Motorola is better than any other available ferrite except for the RCA experimental ferrite shown. In these curves, the large dots indicate experimental points measured by this laboratory for the EAF-2 and Ferrotron materials. Other curves and parts of curves are from descriptive advertising circulars. Note that the RCA ferrites with very high Q at high frequencies also have very low μ properties. This is a common characteristic of ferrites - a very low loss factor usually is accompanied by a low permeability. Nevertheless, it does appear that several of the RCA ferrites are worth investigating for future application in antenna loading. It would be most helpful to have a manufacturing source for some of the RCA ferrites.

VII

FUTURE EFFORT

A complete analysis of the ferrite-loaded log conical spiral antenna will be attempted. It is expected that the ferrite loading of helices will enable a more accurate representation of the parameters to be made. These parameters will then be introduced in the mathematical formulation for the log conical antenna. The loaded zig-zag antenna will be studied in less detail.

Further emphasis will be placed upon magnetic bias control of ferrite antenna elements and upon power handling capability of ferrite antenna elements. Degradation of ferrite antenna radiation characteristics as power level is increased will be considered.

Resumption of the ferrite measurement program is planned for the near future. In order to properly assay the role of ferrite materials, it is necessary to know accurately the critical parameters at the actual operating frequencies. A continuation of this program has been held up, due in part to the unavailability of suitable sizes and shapes of ferrite material. Such shapes have been on order for a considerable time and it is hoped that delivery will be made soon.

In continuing the studies of the loading of traveling wave antennas, it now appears that the prior work can be supplemented by further experimentation on the thickness and placement of ferrite layers. Studies are contemplated on the use of coaxially placed spirals allowing appropriate loading on each spiral. Segmented spirals which are at the same time both coaxial and coplanar allowing independent loading of each segment will also be studied experimentally.

One of the contemplated experiments on the conical log spiral is an inverted spiral used over a ground plane. The intervening space between the ground plane and the spiral will be at least partly filled with a ferrite material. This, in effect,

will give a graduated filling of ferrite material and it will be possible in this way to make a design where the effective distance to the bottom of the cavity (which is the ground plane) will correspond to the optimum distance of the active region at any frequency (i. e. the distance of the active region to the ground plane). In this way it is hoped that it will be possible to make the active region approximately $1/4\lambda$ above the conducting ground plane or the bottom of the cavity which backs the spiral. Other loadings will be made on the conical log spiral using the spiral in the more conventional mode of operation rather than as an inverted spiral as just described.

Experiments to show the variation of performance of antennas over large and small ground planes will be made. These experiments will deal with antennas which should yield information useful in mounting antennas on the edges or flush mounted in aircraft surfaces. Emphasis will be placed on practical antennas such as slots, slot arrays, conical log spirals and planar spirals. Some attention will be given to the effect of non-planar ground planes. Some of the planned future work would extend beyond the end of the present contract.

ACKNOWLEDGEMENTS

Contributors to this report include; Chong K. Rhee, U. Edward Gilreath and R. L. Baker.

REFERENCES

- Adams, A. T. (1964), "The Rectangular Cavity Slot Antenna with Homogeneous Isotropic Loading," The University of Michigan Cooley Electronics Laboratory Report No. 05549-7-T.
- Allen, J. L. (1964), "Array Antennas: New Applications for an Old Technique," IEEE Spectrum, 1, pp. 115-130.
- Bevensee, R. M. (1964), Electromagnetic Slow Wave Systems, John Wiley and Sons, New York.
- Bulgakov, B. M., V. P. Shestopalov, L. A. Shiskin and I. P. Yakimenko (1960), "Symmetrical Surface Waves in a Helix Waveguide with a Ferrite Medium," Radio. i. elek., 5, pp. 102-119.
- Bulgakov, B. M., V. P. Shestopalov, L. A. Shiskin and I. P. Yakimenko, (1961), "The Irreversible Propagation of Waves in a Helix Waveguide Placed in a Ferrite Medium," Radio Eng. and Electronics, 4, pp. 118-134.
- Chatterjee, J. L. (1953), "Radiation Field of a Conical Helix," J. Appl. Phys., 24, pp. 550-559.
- Jasik, H. (1961), Antenna Engineering Handbook, McGraw-Hill, New York, Ch. 9.
- Jones, H. S., Jr. (1965), "Dielectric-Loaded Waveguide Slot Arrays," USAMC Harry Diamond Laboratories Technical Report TR-1269.
- Kornhauser, E. T. (1951), "Radiation Field of Helical Antennas with Sinusoidal Current," J. Appl. Phys., 22, pp. 887-891.
- Kraus, J. D. (1950), Antennas, McGraw-Hill, New York.
- Louisell, W. H. (1960), Coupled Mode and Parametric Electronics, John Wiley and Sons, New York.
- Lyon, J. A. M., et al (1965), "Study and Investigations of a UHF-VHF Antenna," The University of Michigan Radiation Laboratory Report 5549-1-F, AFAL-TR-65-64.
- Pierce, J. R. (1950), Traveling Wave Tubes, D. vanNostrand, Inc., New York.
- Radio Corporation of America (1963), "Hexagonal Magnetic Compounds," RCA Report No. 8, AD 420 336.
- Ramo, S and J. R. Whinnery (1953), Fields and Waves in Modern Radio, John Wiley and Sons, New York. pp. 351, 370 and 371.
- Ramsay, J. F. and B. V. Popovich (1963), "Series-slotted Waveguide Array Antennas," IEEE International Conv. Record, Pt. 1, pp. 30-55.

- Rumsey, V. H. (1953, " Traveling Wave Slot Antennas, " J. Appl. Phys., 24, pp. 1358-1365.
- Shestopalov, V. P. , A. A. Bulgakov and B. M. Bulgakov (1961), "Theoretical and Experimental Investigations of Helix-dielectric Aerials, " Radio.i elek., 6, pp. 159-172.
- Spitz, E. (1962), "A Class of New Type of Broadband Antennas, " Electromagnetic Theory and Antennas, URSI Symposium, Copenhagen , (Ed. E. C. Jordan) Pergamon Press, pp. 1139-1148.
- Thourel, L . (1960), The Antenna, John Wiley and Sons, New York.
- Walter, C.H. (1965) , Traveling Wave Antennas, McGraw-Hill, New York.
- Watkins, D.A. (1958), Topics in Electromagnetic Theory, John Wiley and Sons, New York.
- Weeks, W. L. (1957), "Coupled Waveguide Excitation of Traveling Wave Slot Antennas, " University of Illinois Technical Report No. 27.
- Yakimenko, I. P. and V. P. Shestopalov (1962), "An Experimental Investigation of a Helix Ferrite Waveguide, " Radio Eng. and Electr. Phys., 7, pp.1047-1054.

DOCUMENT CONTROL DATA - R&D

(Security classification of title, body of abstract and indexing annotation must be entered when the overall report is classified)

| | | | |
|---|--|--|-----------------------|
| 1. ORIGINATING ACTIVITY (Corporate author) The University of Michigan Radiation Laboratory Department of Electrical Engineering | | 2a. REPORT SECURITY CLASSIFICATION Unclassified | |
| | | 2b. GROUP | |
| 3. REPORT TITLE Study and Investigation of a UHF-VHF Antenna | | | |
| 4. DESCRIPTIVE NOTES (Type of report and inclusive dates) Interim Report - February through June 1965 | | | |
| 5. AUTHOR(S) (Last name, first name, initial) Lyon, J. A. M. N. G. Alexopoulos, C-C Chen, A. M. Kazi and G. G. Rassweiler | | | |
| 6. REPORT DATE July 1965 | | 7a. TOTAL NO. OF PAGES 63 | 7b. NO. OF REFS 24 |
| 8a. CONTRACT OR GRANT NO. AF 33(615)-2102 | | 9a. ORIGINATOR'S REPORT NUMBER(S) 7140-1-T | |
| b. PROJECT NO. 6278 | | 9b. OTHER REPORT NO(S) (Any other numbers that may be assigned this report) | |
| c. TASK 627801 | | | |
| d. | | | |
| 10. AVAILABILITY/LIMITATION NOTICES Qualified requestors may obtain copies of this report from DDC. | | | |
| 11. SUPPLEMENTARY NOTES | | 12. SPONSORING MILITARY ACTIVITY Air Force Avionics Laboratory AVWE Research and Technology Division, AFSC Wright Patterson AFB, Ohio 45433 | |
| 13. ABSTRACT This report covers the preliminary efforts on the experimental and analytical studies involving the loading of various types of antennas with ferrite material. Major emphasis has been placed upon improvements of conical log spiral antennas through the use of ferrite loading techniques. With this in mind, a series of basic studies on the ferrite loading of helices has been made. These studies indicate the effect of thickness and placement of ferrite material. Data are given showing the shifting of the operating frequency due to the introduction of ferrite material. Also, some information is given on the bandwidth for these study type antennas. A preliminary effort has been devoted to the design of simple slot arrays using ferrite material with provision for magnetic control of these arrays. | | | |

| 14. KEY WORDS | LINK A | | LINK B | | LINK C | |
|---|--------|----|--------|----|--------|----|
| | ROLE | WT | ROLE | WT | ROLE | WT |
| Antennas UHF-VHF Ferrite Loading Techniques | | | | | | |

INSTRUCTIONS

1. **ORIGINATING ACTIVITY:** Enter the name and address of the contractor, subcontractor, grantee, Department of Defense activity or other organization (*corporate author*) issuing the report.
- 2a. **REPORT SECURITY CLASSIFICATION:** Enter the overall security classification of the report. Indicate whether "Restricted Data" is included. Marking is to be in accordance with appropriate security regulations.
- 2b. **GROUP:** Automatic downgrading is specified in DoD Directive 5200.10 and Armed Forces Industrial Manual. Enter the group number. Also, when applicable, show that optional markings have been used for Group 3 and Group 4 as authorized.
3. **REPORT TITLE:** Enter the complete report title in all capital letters. Titles in all cases should be unclassified. If a meaningful title cannot be selected without classification, show title classification in all capitals in parenthesis immediately following the title.
4. **DESCRIPTIVE NOTES:** If appropriate, enter the type of report, e.g., interim, progress, summary, annual, or final. Give the inclusive dates when a specific reporting period is covered.
5. **AUTHOR(S):** Enter the name(s) of author(s) as shown on or in the report. Enter last name, first name, middle initial. If military, show rank and branch of service. The name of the principal author is an absolute minimum requirement.
6. **REPORT DATE:** Enter the date of the report as day, month, year, or month, year. If more than one date appears on the report, use date of publication.
- 7a. **TOTAL NUMBER OF PAGES:** The total page count should follow normal pagination procedures, i.e., enter the number of pages containing information.
- 7b. **NUMBER OF REFERENCES:** Enter the total number of references cited in the report.
- 8a. **CONTRACT OR GRANT NUMBER:** If appropriate, enter the applicable number of the contract or grant under which the report was written.
- 8b, 8c, & 8d. **PROJECT NUMBER:** Enter the appropriate military department identification, such as project number, subproject number, system numbers, task number, etc.
- 9a. **ORIGINATOR'S REPORT NUMBER(S):** Enter the official report number by which the document will be identified and controlled by the originating activity. This number must be unique to this report.
- 9b. **OTHER REPORT NUMBER(S):** If the report has been assigned any other report numbers (*either by the originator or by the sponsor*), also enter this number(s).
10. **AVAILABILITY/LIMITATION NOTICES:** Enter any limitations on further dissemination of the report, other than those

imposed by security classification, using standard statements such as:

- (1) "Qualified requesters may obtain copies of this report from DDC."
- (2) "Foreign announcement and dissemination of this report by DDC is not authorized."
- (3) "U. S. Government agencies may obtain copies of this report directly from DDC. Other qualified DDC users shall request through _____."
- (4) "U. S. military agencies may obtain copies of this report directly from DDC. Other qualified users shall request through _____."
- (5) "All distribution of this report is controlled. Qualified DDC users shall request through _____."

If the report has been furnished to the Office of Technical Services, Department of Commerce, for sale to the public, indicate this fact and enter the price, if known.

11. **SUPPLEMENTARY NOTES:** Use for additional explanatory notes.
12. **SPONSORING MILITARY ACTIVITY:** Enter the name of the departmental project office or laboratory sponsoring (*paying for*) the research and development. Include address.
13. **ABSTRACT:** Enter an abstract giving a brief and factual summary of the document indicative of the report, even though it may also appear elsewhere in the body of the technical report. If additional space is required, a continuation sheet shall be attached.

It is highly desirable that the abstract of classified reports be unclassified. Each paragraph of the abstract shall end with an indication of the military security classification of the information in the paragraph, represented as (TS), (S), (C), or (U).

There is no limitation on the length of the abstract. However, the suggested length is from 150 to 225 words.

14. **KEY WORDS:** Key words are technically meaningful terms or short phrases that characterize a report and may be used as index entries for cataloging the report. Key words must be selected so that no security classification is required. Identifiers, such as equipment model designation, trade name, military project code name, geographic location, may be used as key words but will be followed by an indication of technical context. The assignment of links, rules, and weights is optional.

UNIVERSITY OF MICHIGAN



3 9015 03125 9032